KAERI/TR-1266/99

SSC-K 용 Pool 열수력 분석 모델 개발

Development of Pool Thermal-Hydraulic Analysis Models for SSC-K

한 국 원 자 력 연 구 소

제 출 문

한국원자력연구소장 귀하

본 보고서를 1998 년도 "칼리머 안전해석 기술개발" 과제의 기술보고서로 제출합니다.

1999. 3

과 제 명 : 칼리머 안전해석 기술개발

주 저 자 : 김경두 (칼리머 설계기술개발팀)

공 저 자 : 권영민 (칼리머 설계기술개발팀)

석수동 (칼리머 설계기술개발팀)

장원표 (칼리머 설계기술개발팀)

한도희 (칼리머 설계기술개발팀)

요 약 문

SSC-K (Supper System Code of KAERI)는 한국원자력연구소에서 개발 중인 Pool 형 액체금속로 KALIMER 의 다양한 정상/비정상 조건 및 사고를 분석하기 위한 최적열수력코드이다. SSC-K 는 미국 BNL 에서 Loop 형 액체금속로의 안전해석을 위해 개발된 SSC-L 을 기반으로 개발되었다.

KALIMER 와 같은 Pool 형 원자로는 Loop 형 원자로와 근본적으로 설계개념이 상이하여 KALIMER 안전해석을 위해서는 Loop 형 액체금속로 안전해석을 위해 개발된 SSC-L 의 전반적인 코드 수정이 필요하다. KALIMER 와 일반적인 Loop 형 원자로의 주요 차이는 일차 열전달계통에서 나타난다. KALIMER 에서는 일차 열전달계통을 구성하는 모든 주요기기가 원자로 용기내에 위치하나, Loop 형 원자로에서는 모든 주요기기가 원자로용기 외부에 위치하며 파이프를 통하여 연결되어 있다. 또한 KALIMER 는 일차계통에 하나의 가스 영역이 존재하며 일반적으로 Loop 형 원자로와 같이 가스영역이 펌프탱크와 상부동공으로 분리되지 않는다. KALIMER 는 고온풀과 저온풀이 절연판으로 분리되어 있어 고온풀과 저온풀이 수위가 다르다. 이는 유로에서의 압력강하 및 펌프의 수두에 의해 발생한다. 열제거 기능이 저하되는 사고 발생시에는 고온풀의 수위가 절연판 상부보다 높아져 저온풀로 넘치게 되어 자연순환유로가 형성된다. 이는 피동잔열계통과 같이 열제거 상실사고시 주 열제거형태로 작용한다. KALIMER 는 Loop 형 원자로와 달리 관파단 사고의 발생은 펌프배출파이프에서만 가능하고, 이 파이프도 저온풀에 잠겨 있어 파단유량은 감소한다. 중간 열전달계통과 증기발생기계통은 Loop 형 원자로와 일반적으로 동일하다.

위에서 지적한 KALIMER 와 같은 Pool 형 원자로의 차이를 반영하기 위해 SSC-L 코드를 전반적으로 수정하여 KALIMER 안전해석에 적합한 SSC-K 를 개발하였다. 개발된 모델은 시험계산을 통하여 정성적으로 타당한 예측능력이 있음을 확인하였다. 개발된 SSC-K 코드는 향후 KALIMER 안전해석에 사용할 수 있을 것으로 사료되며, 이를 위해서는 개발된 모델에 대한 충분한 검증작업이 이루어져야 한다.

SUMMARY

The Supper System Code of KAERI (SSC-K) is a best-estimate system code for analyzing a variety of off-normal or accidents in KALIMER which is a pool type LMR. It is developed at Korea Atomic Energy Research Inititution on the basis of SSC-L developed at BNL to analyze loop-type LMR transients.

Because of inherent difference between the pool and loop design, the major modification of SSC-L is required for the safety analysis of KALIMER. The major difference between KALIMER and general loop type LMRs exists in the primary heat transport system. In KALIMER, all of the essential components consisted of the primary heat transport system are located within the reactor vessel. This is contrast to the loop type LMRs, in which all the primary components are connected via piping to form loops attached externally to the reactor vessel. KALIMER has only one cover gas space. This eliminates the need for separate cover gas systems over liquid level in pump tanks and upper plenum. Since the sodium in hot pool is separated from cold pool by insulated barrier in KALIMER, the liquid level in hot pool is different from that in the cold pool mainly due to hydraulic losses and pump suction heads occuring during flow through the circulation pathes. In some accident conditions, the liquid in the hot pool is flooded into cold pool and it forms the natural circulation flow path. During the loss of heat sink transients, this will provided as a major heat rejection mechanism with the passive decay heat removel system. Since the pipes in the primary system exist only between pump discharge and core inlet plenum and are submerged in cold pool, a pipe rupture accident becomes less severe due to a constant back pressure exerted against the coolant flow from break. The intermediate and steam generator systems of both designs are generally identical.

To adapt SSC-K to KALIMER design, the major modification of SSC-L has been made for the safety analysis of KALIMER. Test runs have been performed for the qualitative verification of the developed models. The present work would make it possible to use SSC-K for the priliminary safety analysis of KALIMER. However, the further validation of SSC-K is required to be used for real applications.

Table of Contents

제출문 i

요약문 ii

Summary iii

Table of Contents iv

List of Tables v

List of Figures vi

1. Introduction 1

2. Steady-State Models 6

2.1 Global Heat Balance 6

2.1.1 Steady-State Calculation in IHX 8

2.2 Hot Pool Pressure Distribution 13

2.3 Thermal-Hydraulics for Fuel Assembly Region 14

2.3.1 Core Thermal-Hydraulics 14

2.3.2 Core Pressure Distribution 16

2.3.3 Upper Plenum Thermal-Hydraulics 20

2.3.4 Core Outlet Module Hydraulics 22

2.4 Loop Hydraulics 23

2.4.1 Hydraulics for IHX 23

2.4.2 Hydraulics for Pipes 25

2.4.3 Pump 26

2.4.4 Pressure Distribution of Pipes 27

2.4.5 Cold Pool Hydraulics 27

3. Transient Models 29

3.1 Flow Equations 29

3.1.1 Intact System 29

3.1.2 Damaged System 31

3.2 Pump Suction Pressure 32

3.3 Liquid Levels in Pools 34
3.4 Reactor Internal Pressure 35
3.4.1 Intact System 36
3.4.2 Damaged System 38
3.5 Energy Balance in Hot Pool 40
3.5.1 Lower Mixing Zone 41
3.5.2 Upper Mixing Zone 43
3.5.3 Other Temperatures in hot pool 45
3.6 Energy Balance in Cold Pool 46

4. Model Verifications 50
4.1 Null Transient Calculation 50
4.2 Transient Simulations 51
4.2.1 Unprotected Loss of Heat Sink (ULOHS) 51
4.2.2 Overflow Simulation 55
4.2.3 Overflow/Break Simulation 58

5. Conclusions and Future Work 61

References 62

Appendix A. Input Changes 63
Appendix B. Code Modification List 67

List of Figures

1.1 KALIMER Primary System 3
1.2 Primary System Schematics 4
1.3 Schematic diagram of KALIMER System 5
2.1 Flowchart for Steady-State Calculation 7
2.2 Steady-State Conditions for an IHX Nodal Section 9
3.1 Flowchart for Transient Calculation 30
3.1 Schematic of SSC-K Modeling for KALIMER 33
3.2 Two Mixing Zone Model for Hot Pool 41
4.1 Temperatures for case 1 (ULOHS) 52
4.2 Temperatures for case 2 (ULOHS) 53
4.3 Sodium Levels for case 1 (ULOHS) 53
4.4 Sodium Levels for case 2 (ULOHS) 54
4.5 Reactivity for case 1 (ULOHS) 54
4.6 Reactivity for case 2 (ULOHS) 55
4.7 Reactivity (Overflow/ULOHS) 56
4.8 Sodium Temperatures (Overflow/ULOHS) 57
4.9 Sodium Levels (Overflow/ULOHS) 57
4.10 Mass Flow Rates (Overflow/ULOHS) 58
4.11 Sodium Temperatures (Break/Overflow/ULOHS) 59
4.12 Sodium Levels (Break/Overflow/ULOHS) 60
4.13 Mass Flow Rates (Break/Overflow/ULOHS) 60
A.1 Pipes 65

List of Tables

4.1 Major Parameters for Nominal Operating Condition 50

A.1 Elevation of Each Pipe Exit for Primary Loop 67

B.1 Code Modification List 67

1. INTRODUCTION

The Supper System Code of KAERI (SSC-K) is a best-estimate system code for analyzing a variety of off-normal or accidents in KALIMER which is a pool type design (Fig. 1.1). It is developed at Korea Atomic Energy Research Inititution (KAERI) on the basis of SSC-L developed at BNL to analyze loop-type LMR transients. Because of inherent difference between the pool and loop design, the major modifications of SSC-L has been made for the safety analysis of KALIMER.

The major difference between KALIMER and general loop type LMRs exists in the primary heat transport system as shown in Fig. 1.2. In KALIMER, all of the essential components consisted of the primary heat transport system are located within the reactor vessel. This includes reactor, four EM pumps, primary side of four intermediate heat exchangers, sodium pools, cover gas blanket, and associated pipings. This is contrast to the loop type LMRs, in which all the primary components are connected via piping to form loops attached externally to the reactor vessel. KALIMER has only one cover gas space. This eliminates the need for separate cover gas systems over liquid level in pump tanks and upper plenum. The IHX outlet is directly connected to cold pool instead of the piping into pump suction which is a typical configuration in loop type LMRs. Since the sodium in hot pool is separated from cold pool by insulated barrier in KALIMER, the liquid level in hot pool is different from that in the cold pool mainly due to hydraulic losses and pump suction heads occuring during flow through the circulation pathes. In some accident conditions the liquid in the hot pool is flooded into cold pool and it forms the natural circulation flow path. During the loss of heat sink transients, this will provided as a major heat rejection mechanism with the passive decay heat removel system. Since the pipes in the primary system exist only between pump discharge and core inlet plenum and are submerged in cold pool, a pipe rupture accident becomes less severe due to a constant back pressure exerted against the coolant flow from break. The intermediate and steam generator systems of both designs are generally identical (Fig. 1.3).

The SSC-K is designed to predict plant response under various off-norrmal and

accident conditions until sodium boiling occurs. This code can also perform the steady-state initialization. This feature is provided so that user can easily obtain the various preaccident initial conditions based on user-specified design parameters and minimum operating values.

A comprehensive description of models is given in following Sections; the models for the steady-state initialization is described in Section 2 and the transient modeling is discussed in Section 3. In Section 4, the verification results to illustrate the code modeling capability against pool-type LMR have been included. In last Section, the conclusions and action items for further development effort are discussed. Appendices presents a summary of additional input requirements compare to SSC-L and the cautions needed for KALIMER modeling. Since SSC-K is developed on the basis of SSC-L, many portions of SSC-K utilized the same methods and models as its parent code SSC-L. Therefore, the primary emphasis in the development and its description in the report has been focus on the differences between the two codes.

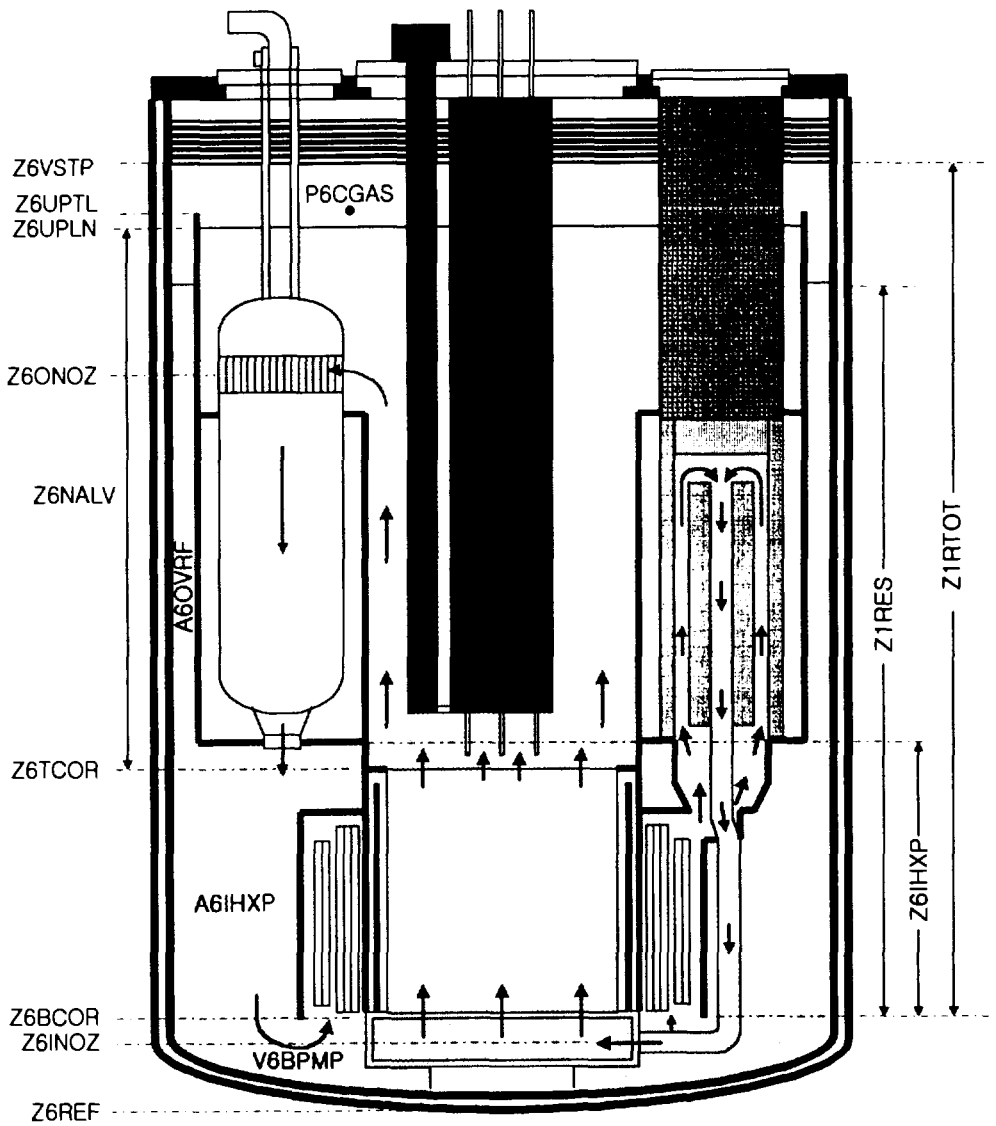

Fig. 1.1: KALIMER Primary System

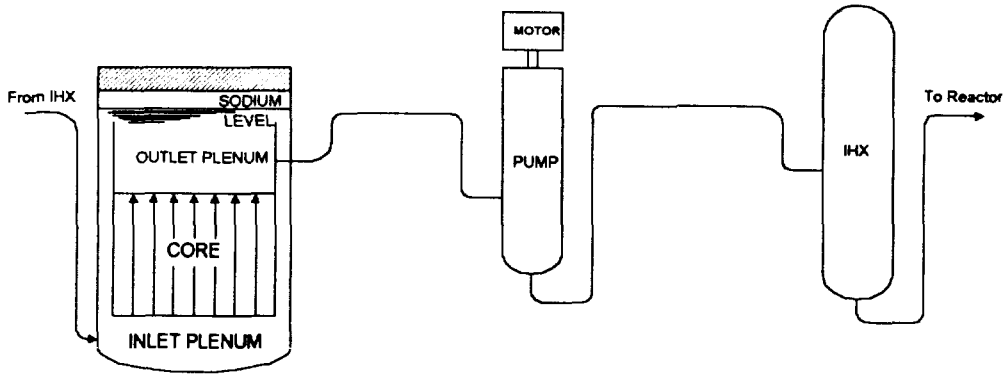

(a) Loop-type LMR

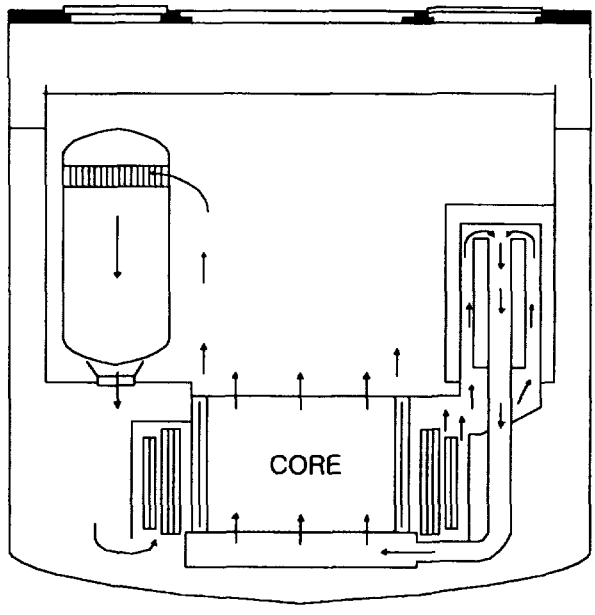

(b) KALIMER

Fig. 1.2: Primary System Schematics

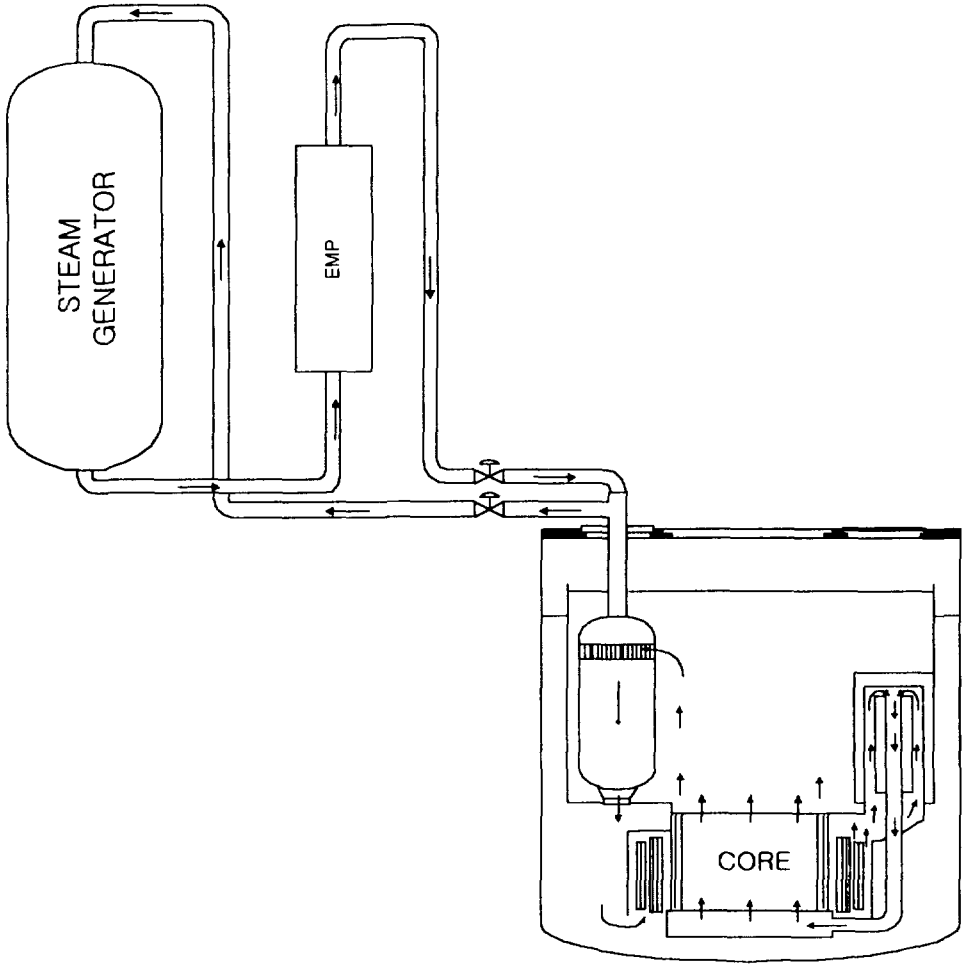

Fig. 1.3: Schematic diagram of KALIMER System

2. STEADY-STATE MODELS

In the initial part of the transient calculation, a stable and unique steady state or pre-transient solution for entire plant must be obtained. As a result, the continuity, energy, and momentum conservation equations in time-independent form are reduced to a set of nonlinear algebraic equations. These equations are solved in two steps. First, the global parameters are obtained. More detailed characterization is achieved by using the global conditions obtained in the first step, as boundary conditions. Since the SSC-K is developed based on SSC-L, the most of the steady-state routine in SSC-L is used with minimum changes. Some modifications are required due to including the cold pool model into SSC-K. The flow chart for steady-state solution routine is in Fig. 2.1.

2.1 Global Heat Balance (PBAL9S)

At steady state, the fluid and metal in the core inlet plenum are assumed to be thermal equilibrium. The temperatures are then equal to the user specified fluid temperature at the inlet nozzle, i.e.,

$$T_{lplenum} = T_{metal} = T_{6inlt}$$

The core inlet temperature is specified as input. The hot pool sodium enthalpy and temperature can be obained using known values of core power and mass flow rate:

$$h_{6outl} = h_{6inlt}(T_{6inlt}) + P_{core} / W_{6tot}$$

$$T_{6outl} = f(h_{6outl})$$

The IHX inlet and outlet temperatures are determined according to the location of pump in order to account the temperature rise due to pump heat generation.

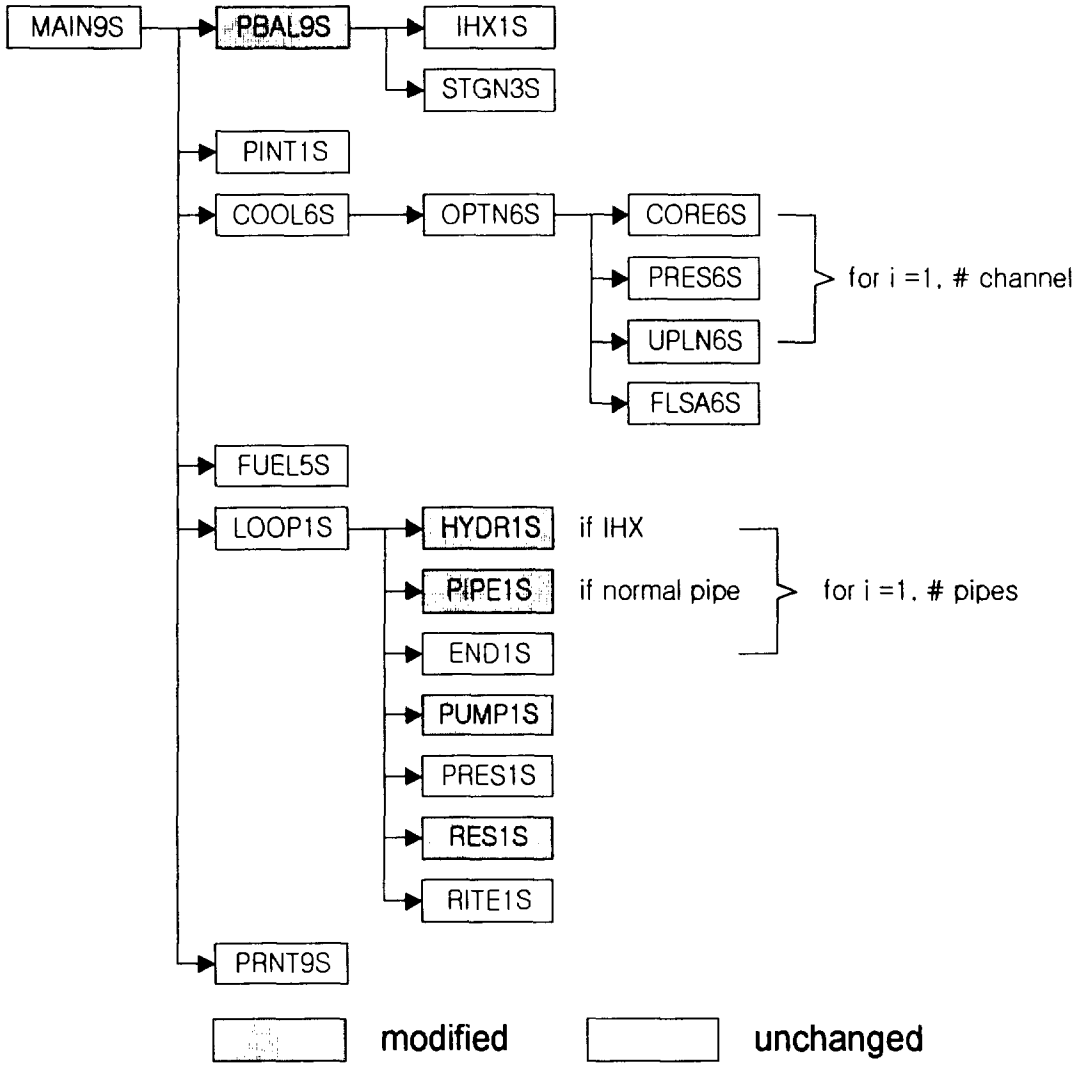

Fig. 2.1: Flowchart for Steady-State Calculation

$$\begin{cases} T_{INIHX} = T_{6outl} + \Delta T_{l\,pump} & \text{if pump is between hot pool and IHX} \\ T_{INIHX} = T_{6outl} & \text{if pump is located after IHX} \end{cases}$$

$$\begin{cases} T_{OUHX} = T_{6inlt} - \Delta T_{l\,pump} & \text{if pump is between IHX and core inlet plenum} \\ T_{OUHX} = T_{6inlt} & \text{if pump is located before IHX} \end{cases}$$

The total heat removal rate by IHX can be calculated as following:

$$Q_{TOINT} = W_{loop}[h(T_{INIHX}) - h(T_{OUHX})]$$

2.1.1 Steady State Calculation in IHX (PBAL9S → IHX1S)

To start the steady state calculations for IHX, the boundary temperatures at one end of IHX, in this case T_{1INHX}, T_{2IHXO} and W_{2loop}, must been known. T_{INHX} is known from global thermal balance calculations. The IHX outlet temperature and flow rate for intermediate side are guessed for first pass:

$$\begin{cases} W_{2loop} = W_{1loop} + 1.0 \\ T_{2IHXO} = T_{1INHX} - 20 \end{cases} \qquad \text{where } T_{2IHXI} = \text{known}$$

The iteration procedure for the temperature distribution of IHX is as following:

Step 1. Find out the node length and heat transfer areas for tube and shell sides:

Δx : length of IHX node

A_2 : primary side (shell side) heat transfer area for each IHX node

$= \pi \cdot (IHX\ tube\ outer\ diameter) \cdot \Delta x \cdot (\#\ tubes)$

A_1 : intermediate side (tube side) heat transfer area for each IHX node

Step 2. Compute the constants for computation of Peclet numbers:

$$A_{PEP} = (diameter)(velocity)(density) = P_e \cdot k / c_p = \frac{W_{1loop} \cdot d_1}{A_{1IHX}}$$

$$A_{PES} = (diameter)(velocity)(density) = P_e \cdot k / c_p = \frac{W_{2loop} \cdot d_2}{A_{2IHX}}$$

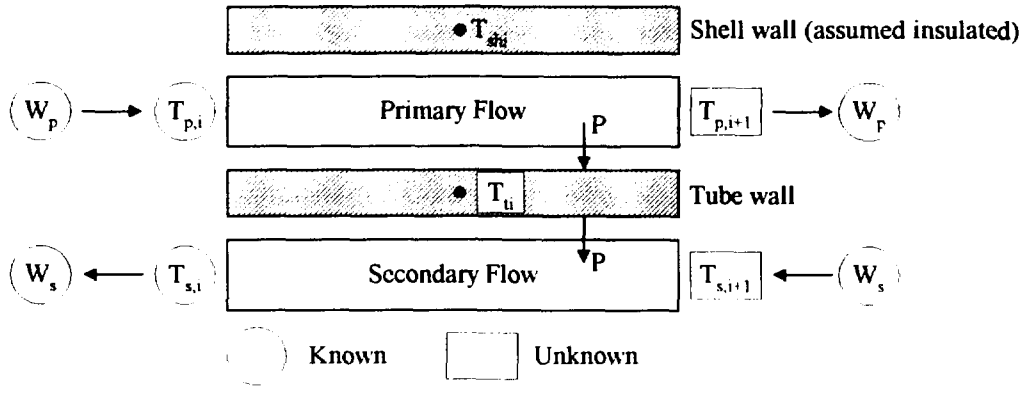

Fig. 2.2: Steady state conditions for an IHX nodal section

Step 3. Guess the tube structure temperature (Fig. 2.2):

$$TT = \frac{T_{i,p} + T_{i,s}}{2}, \quad T_{po} = T_{pi}, \quad T_{so} = T_{si}$$

Step 4: Calculate the node average sodium temperatures:

$$\overline{T}_p = \frac{T_{po} + T_{pi}}{2}, \quad \overline{T}_s = \frac{T_{so} + T_{si}}{2}$$

Step 5: Find out the non-dimensional numbers for heat transfer coefficients:

Peclet numbers for primary and intermediate sides

$$P_{ep} = A_{PEP} \cdot c_{p_p} / k_p, \quad P_{es} = A_{PES} \cdot c_{p_s} / k_s$$

Nusselt number

$Nu_p = a + b \cdot P_e^c$ Shell side (primary)

$Nu_s = 6.0 + 0.025 \cdot (\overline{\Psi} P_{es})^{0.8}$ Aoki's correlation for tube side (intermediate)

where $\overline{\Psi} = \dfrac{0.014(1 - e^{-71.8x})}{x}$

$$x = \frac{1}{Re_s^{0.45} \cdot Pr_s^{0.2}}$$

$$Re_s = \frac{\rho u d}{\mu} = \frac{A_{PES}}{\mu_s}$$

$$Pr_s = \frac{\nu}{\alpha} = \frac{c_{p_s} \cdot \mu_s}{k_s}$$

Step 6: Calcualte the overall heat transfer coefficients:

$$U_{pt} = \frac{1}{\dfrac{D_{h,p}}{Nu_p \cdot k_p} + r_{wall,p} + r_{foul,p}}$$

$$U_{st} = \frac{1}{\frac{D_{h,s}}{Nu_s \cdot k_s} + r_{wall,s} + r_{foul,s}}$$

Step 7: Calculate the node outlet temperatures for primary and intermediate sides:

$$e_{po1} = e_{pi} + \frac{A_2 \cdot U_{pt}(TT - \overline{T}_p)}{W_{1loop}}$$

$$e_{so1} = e_{si} + \frac{A_1 \cdot U_{st}(TT - \overline{T}_s)}{W_{2loop}}$$

$$T_{po1} = T(e_{po1})$$

$$T_{so1} = T(e_{so1})$$

Step 8: Calculate the node average sodium temperatures and tube temperature based on the calculated node exit temperatures:

$$\overline{T}_p = \frac{T_{po1} + T_{pi}}{2}$$

$$\overline{T}_s = \frac{T_{so1} + T_{si}}{2}$$

$$TT_1 = \frac{A_1 U_{st} \overline{T}_s + A_2 U_{pt} T_p}{A_1 U_{st} + A_2 U_{pt}}$$

Step 9: Perform the convergence test for the node:

if $\left|T_{po} - T_{po1}\right| > \varepsilon$ and $\left|T_{so} - T_{so1}\right| > \varepsilon$ and $\left|TT - TT_1\right| > \varepsilon$ then

$$T_{pol} \rightarrow T_{po},\ T_{sol} \rightarrow T_{so},\ TT_l \rightarrow TT$$

go to Step 4 and iterate again.

Step 10: Reset the node exit temperatures into the inlet temperatures for next node until $i = nihxl$:

$T_{pol} \rightarrow T_{pi}$, $T_{sol} \rightarrow T_{si}$, $TT_l \rightarrow TT$ and go to Step 4 and continue for next node.

Step 11. Perform the error checking if the energy gain is equal to energy loss:

$$T_{1OUHX} = T(e_{po})$$

$$T_{2INHX} = T(e_{so})$$

$$Q_{1loss} = W_{1loop}(e_{p,in} - e_{po})$$

$$Q_{2gain} = W_{2loop}(e_{s,out} - e_{s,in})$$

if $\left| 1 - \frac{Q_{2gain}}{Q_{1loss}} \right| > \varepsilon$ error

Step 12. Check for convergence based on total energy balance:

The heat rejection from IHX should equal to the reactor heat plus heat addition at the pump within specified limits:

if $\left| \frac{Q_{TOINT} - Q_{2gain}}{Q_{TOINT}} \right| < \varepsilon$ quit interation

Step 13. If not, the secondary outlet temperature and flow rate have to be reselected and the computation repeated until convergence is obtained:

Log-mean temperature difference

$$\Delta\overline{T} = \frac{(T_{1OUHX} - T_{2INHX}) - (T_{1INHX} - T_{2OUHX})}{ln[(T_{1OUHX} - T_{2INHX}) / (T_{1INHX} - T_{2OUHX})]}$$

$$UA = Q_{2gain} / \Delta\overline{T}$$

Assuming UA constant, determine new *lmtd* guess

$$\Delta\overline{T}_{new} = Q_{TOINT} / UA$$

$$\Delta T_A = T_{1OUHX} - T_{2INHX}$$

$$\Delta\overline{T}_{new} = \frac{\Delta T_A - \Delta T_B}{ln[\Delta T_A / \Delta T_B]} \quad \rightarrow \text{Find } \Delta T_B \text{ using root finding scheme.}$$

$$T_{2OUHX} = T_{1INHX} - \Delta T_B$$

$$W_{2loop} = \frac{Q_{TOINT}}{[e(T_{2OUHX}) - e(T_{2INHX})]} \quad \text{Return to Step 1}$$

After calculating the temperature distribution of IHX, the similar process is performed for the energy balance for steam generator.

2.2 Hot Pool Pressure Distribution (PINT1S)

Subroutine PINT1S calculates the interface pressure between the hot pool and IHX.

$$P_{11NLT} = P_{6CGAS} + \rho(T_{6OUTL}) \cdot g(Z_{6UPLN} - Z_{6ONOZ})$$

where Z_{6UPLN} : relative height of sodium in vessel upper plenum to Z_{6REF}

Z_{6ONOZ} : elevation of vessel outlet nozzle above Z_{6REF}

$$T_{11NLT} = T_{6OUTL}$$

$$P_{6OUTL} = P_{11NLT}$$

$$P_{6INTL} = P_{6OUTL} + P_{1PDRV}$$

where P_{1PDRV} : pressure drop between core inlet and IHX inlet

2.3 Thermal-Hydraulics for Fuel Assembly Region (COOL6S)

2.3.1 Core Thermal-Hydraulics (CORE6S)

The core region is divided into *N6CHAN* parallel channels. These channels represent either fuel, blanket, or control rods. The flow rate for each channel is obtained by user specified flow fraction of the total flow through these channels.

$$W_{6CHAN_j} = W_{6TOT} \cdot F_{6FLOW_j}$$

$$G_{61_j} = \frac{W_{6CHAN_j}}{N_{6RODS_j} \cdot A_{6ROD_j}}$$

where G_{61_j} : mass flux of channel j

N_{6RODS_j} : number of rods in channel j

A_{6ROD_j} : sodium flow area per rod in channel j

Each of the flow channels is divided into a user-controlled number of axial slices. The axial distributions of coolant enthalpy and pressure in all channels are determined in this subroutine.

$$F_{CONS1} = \frac{P_{6TPOW} \cdot F_{6TPOW_j}}{Z_{6CHAN} \cdot W_{6CHAN_j}}$$

where F_{6TPOW_j} : Total normalized power fraction in channel j from fission and decay heating

$$Q_{FACT_{ji}} = \frac{dh}{dz}\Delta z = \frac{1}{W_{6CHAN_j}} \frac{P_{6TPOW} \cdot F_{6TPOW_j} \cdot F_{6NPWA_{ji}} \cdot Z_{6DELT_{ji}}}{Z_{6CHAN} \cdot}$$
$$= F_{CONS1} \cdot F_{6NPWA_{ji}} \cdot Z_{6DELT_{ji}}$$

where $Q_{FACT_{j,i}}$: enthalpy change in axial slice i of channel j

$F_{6NPWA_{j,i}}$: normalized axial power in axial slice i of channel j

$Z_{6DELT_{j,i}}$: length of axial slice i in channel j

$$T_{AVG} = \frac{T_{in} + T_{OLD}}{2}$$

$$T_{OUT} = T_{in} + Q_{FACT_{ji}} / C_p(T_{AVG})$$

where T_{in} : inlet temperature of axial slice i in channel j (known)

T_{OLD} : outlet temperature of axial slice i in channel j (unknown)

T_{OUT} : calculated outlet temperature of axial slice i in channel j

if the temperature difference between initial guessing value and calculated value, $|T_{OUT} - T_{OLD}|$, is greater than user specified limit, T_{OLD} is reseted to T_{OUT} and T_{OUT} is calculated again unitl $|T_{OUT} - T_{OLD}|$ is less than the limit. Then, the friction and heat transfer

coefficients are calculated based upon the new outlet temperature of the axial slice.

$$f_{6FRIC_{JJ}} = f\left[D_h, G_{61_J}, \mu(T_{OUT}), (P/D)_{rod}, (P/D)_{wire\ wrap}, L_{6ATYP}\right]$$

$$h_{6NODE_{JJ}} = \frac{Nu\left[D_h, G_{61_J}, T_{AVG}, (P/D)_{rod}\right] \cdot K(T_{AVG})}{D_h}$$

After completing the calculations for the current axial slice, the same calculations performs for the next axial slice.

2.3.2 Core Pressure Distribution (PRES6S)

Because the current version of SSC-K simulates single phase flow, the flow is assumed to be incompressiable. The axial distributions of coolant pressure in all channels are determined by momentum equations.

The pressure of the core bottom is obtained from the pressure of core inlet plenum by substracting the pressure drop due to form loss and gravitational loss:

$$G_{LPLN} = W_{6TOT} / A_{6LPLN}$$

$$\Delta P^{LP}_{grav} = \rho g \cdot (Z_{6BCOR} - Z_{6INOZ})$$

$$\Delta P^{LP}_{loss} = -F_{6PKLP}$$

where G_{LPLN} : mass flux of lower plenum

ΔP^{LP}_{grav} : gravitation pressure drop from inlet nozzle to bottom of core

ΔP^{LP}_{loss} : pressure drop due to form loss from inlet nozzle to bottom of core

F_{6PKLP} : user specified pressure drop due to form loss from inlet nozzle to bottom

of core

$$P_{6BCOR} = P_{6INLT} - \Delta P_{loss}^{LP} - \Delta P_{grav}^{LP}$$

$$K_{6LP} = 2\rho \cdot \Delta P_{loss}^{LP} / (G_{LPLN} \cdot |G_{LPLN}|)$$

where P_{6BCOR} : Pressure of the core bottom

K_{6LP} : equivalent form loss coef. from inlet nozzle to bottom of core

The pressure of the core top is obtained from the cover gas pressure by adding the pressure drop due to form loss and gravitational loss:

$$G_{UPLN} = W_{6TOT} / A_{6UPLF}$$

$$\Delta P_{grav}^{UP} = \rho g \cdot (Z_{6UPLN} - Z_{6TCOR})$$

$$\Delta P_{loss}^{UP} = -F_{6PKUP}$$

where G_{UPLN} : mass flux of upper plenum

ΔP_{grav}^{UP} : gravitation pressure drop from top of core to top of hot pool

ΔP_{loss}^{UP} : pressure drop due to form loss from top of core to top of hot pool

F_{6PKUP} : user specified pressure drop due to form loss from top of core to top of hot pool

$$P_{6TCOR} = P_{6CGAS} + \Delta P_{grav}^{UP} + \Delta P_{loss}^{UP}$$

$$K_{6UP} = 2\rho \cdot \Delta P_{loss}^{UP} / (G_{UPLN} \cdot |G_{UPLN}|)$$

where P_{6TCOR} : Pressure of the core bottom

K_{6UP} : equivalent form loss coef. from inlet nozzle to bottom of core

Before calculating the pressure distribution for the active core region, the pressre drop in inlet orifice zone has to be estimated:

$$\Delta P_{grav}^{INOZ} = \rho g \Delta Z_{6INZ}$$

$$W_{INOZ_j} = \frac{W_{6TOT} \cdot F_{6FLOW_j}}{N_{5ASSY_j}}$$

where ΔP_{grav}^{INOZ} : Pressure drop for inlet orifice zone

W_{INOZ_j} : flow rate per subassembly for channel j

F_{6FLOW_j} : flow fraction for channel j

Because the pressure drop due to friction in inlet orifice zone is given by user, the hydraulic diameter for orifice zone can be found by Bisection or Newton's method (YHYD6S).

1. Guess the initial value for D_h^n

3. Calculate the pressure drop due to friction

$$\Delta P_{fric}^{calc} = f(D_h, G, \mu) \frac{\Delta Z_{6INZ}}{D_h} \frac{G|G|}{2\rho}$$

4. Find the difference between user specified pressure drop and calculated pressure drop

$$\Delta P^{n+1} = \Delta P_{fric}^{INOZ} - \Delta P_{fric}^{calc}$$

5. Reset the upper and lower limits for Bisection method.

$$\begin{cases} \Delta P^{UP} = \Delta P^{n+1} & \text{if } \Delta P^{n+1} > 0.0 \\ \Delta P^{LOW} = \Delta P^{n+1} & \text{if } \Delta P^{n+1} < 0.0 \end{cases}$$

6. Convergence test

if $\Delta P^{n+1} < 1.0$ then $D_h^{INOZ} = D_h$ and terminate the iteration

7. Find the hydraulic diameter for next iteration:

$$D_h^{n+1} = D_h^n + \Delta P^n \left| \frac{D_h^{n-1} - D_h^n}{\Delta P^n - \Delta P^{n-1}} \right|$$

8. Test if D_h^{n+1} is within the bounds.

$$\begin{cases} \text{Reset the values and return to step2} & \text{if } D_h^{LOW} < D_h^{n+1} < D_h^{UP} \\ D_h^{n+1} = \dfrac{D_h^{LOW} + D_h^{UP}}{2} & \\ \quad \text{Reset the values and return to step2} & \text{else} \end{cases}$$

Because the form loss coefficient due to expansion and contraction in inlet orifice zone is given by user, the pressure drop in orifice zone can be obtained such as:

Mass flux for inlet orifice zone is obtained from the calculated hydraulic diameter:

$$G_{INOZ} = \frac{4 \cdot W_{INOZ}}{\pi \cdot D_h^{INOZ}}$$

The pressure drop drop to form loss:

$$\Delta P_{loss}^{INOZ} = F_{6LSA} \cdot \frac{G_{INOZ} \cdot |G_{INOZ}|}{2\rho}$$

The pressure at the bottom of active core region is:

$$P_{6NODE_{j,1}} = P_{6BCOR} - \Delta P_{grav}^{INOZ} - \Delta P_{loss}^{INOZ} - \Delta P_{fric}^{INOZ}$$

The constant for calculation of the pressure distribution in active core region:

$$\rho_{j,\Delta i} = \frac{\rho_{j,i} + \rho_{j,i+1}}{2}$$

where $\rho_{j,\Delta i}$: average density for nodes i and $i+1$ in channel j

$$\Delta P_{j,\Delta i}^{grav} = \rho_{j,\Delta i} g \Delta Z_{j,\Delta i}$$

$$\Delta P_{j,\Delta i}^{fric} = f_{6FRIC} \frac{\Delta Z_{j,\Delta i}}{D_h} \frac{G_{61}|G_{61}|}{2\rho_{j,\Delta i}}$$

$$\Delta P_{j,\Delta i}^{mflux} = \frac{G_{61}^2}{\rho_{j,i+1}} - \frac{G_{61}^2}{\rho_{j,i}}$$

The pressure at node $i+1$ is:

$$P_{6NODE_{j,i+1}} = P_{6NODE_{j,i}} - \Delta P_{j,\Delta i}^{grav} - \Delta P_{j,\Delta i}^{fric} - \Delta P_{j,\Delta i}^{mflux}$$

2.3.3. Upper Plenum Thermal-Hydraulics (UPLN6S)

The core region is divided into *N6CHAN* parallel channels. These channels represent either fuel, blanket, or control rods. The flow rate for each channel is obtained by user specified flow fraction of the total flow through these channels.

$$W_{6CT} = \sum_{j}^{N6CHAN} W_{6CHAN_j}$$

$$E_{6AVER} = \sum_{j}^{N6CHAN} \left(W_{6CHAN_j} \cdot E_{6NODE_j}\right) \Big/ W_{6CT}$$

$$T_{AVER} = \left(\sum_{j}^{N6CHAN} T_{6NODE_j} \right) \Big/ N_{6CHAN}$$

$$Q_{IN} = \sum_{j}^{N6CHAN} \left(W_{6CHAN_j} \cdot E_{6NODE_j}\right)$$

The temperatures for cover gas, internal structure, thermal liner and vessel closure head can be found by solving the governing energy equations for hot pool region by iterative procedure:

1. Guess thermal liner temperature, T_{6M2} same as hot pool sodium temperature:

$$T_{6M2} = T_{6OUTL}; \quad T_{UP} = T_{6OUTL}; \quad T_{LOW} = -1.$$

$$E_{6BPUI} = E_{6BPLI}; \quad T_{6BPUI} = T(E_{6BPUI})$$

2. Compute the temperatures for cover gas, internal structure, thermal liner from user-specified heat transfer coefficients and the assmued thermal liner temperature:

$$T_{6CGAS} = T_{6M2} - U_{ALM2}(T_{6OUTL} - T_{6M2})/U_{AGM2}$$

$$T_{6M3} = \left(U_{AGM3} T_{6CGAS} + U_{AGM3} T_{6BPUI}\right) / 2 \cdot U_{AGM3}$$

$$T_{6M1} = \left(U_{ALM1} T_{6OUTL} + U_{AGM1} T_{6CGAS}\right) / \left(U_{ALM1} + U_{AGM1}\right)$$

3. Compute T_{6M2}

$$T^{*}_{6M2} = T_{6CGAS} - \frac{U_{ALGL}\left(T_{6OUTL} - T_{6CGAS}\right) + U_{AGM1}\left(T_{6M1} - T_{6CGAS}\right) + U_{AGM3}\left(T_{6M3} - T_{6CGAS}\right)}{U_{AGM2}}$$

4. If computed T^{*}_{6M2} is not equal to assumed T_{6M2}, reset and iterate.

In order to calculate the pressure drop for outlet module, the core outlet pressure has to be found.

$$P_{6OUTL} = P_{6CGAS} + \rho(T_{6OUTL}) g \cdot \left(Z_{6UPLN} + Z_{6ONOZ}\right)$$

$$P_{6TCOR} = P_{6OUTL} + \rho(T_{6OUTL}) g \cdot \left(Z_{6ONOZ} + Z_{6TCOR}\right)$$

where P_{6OUTL} : IHX inlet pressure

P_{6TCOR} : core outlet pressure

2.3.4 Core Outlet Module Hydraulics (FLSA6S)

This subrutine calculates the pressure equalization loss coefficient at outlet module.

$$W_{INOZ_j} = W_{6TOT} \cdot F_{6FLOW_j} / N_{5ASSY_j}$$

$$G_{OUZ_j} = W_{INOZ}/(A_{6ROD_j} \cdot N_{5AROD_m})$$

where W_{INOZ_j} : flow rate per assembly in channel j

G_{OUZ_j} : mass flux per assembly in channel j

$$\Delta P^{OUT}_{grav_j} = \rho \cdot g \cdot \Delta Z_{6OUZ}$$

$$\Delta P^{OUT}_{kloss_j} = \frac{F_{6LSA_j}}{2} \frac{G_{OUZ_j}\left|G_{OUZ_j}\right|}{\rho}$$

where $\Delta P^{OUT}_{kloss_j}$: pressure drop for outlet module zone in channel j due to contraction and expansion

F_{6LSA_j} : k-loss factor for outlet module zone in channel j due to contraction and expansion

$$\Delta P_\varepsilon = P_{6NODE_{lastnode}} - P_{6TCOR} - \Delta P^{OUT}_{grav_j} - \Delta P^{OUT}_{kloss_j}$$

$$K_{OUT_j} = F_{6LSA4_j} = 2 \cdot \Delta P_\varepsilon \cdot \rho / (G_{OUZ_j} \cdot \left|G_{OUZ_j}\right|)$$

where F_{6LSA4_j}: k-loss factor for outlet module in channel j except k-loss due to expansion and contraction

2.4 Loop Hydraulics (LOOP1S)

2.4.1 Hydraulics for IHX (HYDR1S)

This subroutine solves the steady state pressure drop and/or k-loss factor for the IHX.

The pressure drop due to flow differnece:

$$\Delta P_{frow} = \left(\frac{1}{\rho_{IHX,O}} - \frac{1}{\rho_{IHX,I}} \right) \frac{W_{IHX}|W_{IHX}|}{A_{IHX}^2}$$

$$Re = \frac{W \cdot De}{A_x \cdot \mu}$$

$$f = f(Re)$$

The pressure drop due to wall friction:

$$\Delta P_{fric} = f \frac{\Delta x}{D_h} \frac{W_{IHX}|W_{IHX}|}{2\rho \cdot A_{IHX}^2}$$

The pressure drop due to gravitation:

$$\Delta P_{grav} = g\left(\rho_{IHX,I} \cdot \sin\phi_{IHX,I} \Delta x_{IN} + \rho_{IHX,O} \cdot \sin\phi_{IHX,O} \Delta x_{OUT} + \sum_{i}^{N_{INODE}} \rho_i \cdot \sin\phi_i \Delta x_i \right)$$

The pressure drop due to contraction or expansion at IHX inlet:

$$\Delta P_{loss,in} = K_{in} \frac{W_{IHX}|W_{IHX}|}{2\rho_{in} \cdot A_{in}^2}$$

The pressure drop due to contraction or expansion at IHX outlet:

$$\Delta P_{loss,out} = K_{out} \frac{W_{IHX}|W_{IHX}|}{2\rho_{out} \cdot A_{out}^2}$$

The total pressure drop except the pressure drop due to k-loss factor inside IHX:

$$\Delta P_{SUM} = \Delta P_{flow} + \Delta P_{fric} + \Delta P_{grav} + \Delta P_{loss,in} + \Delta P_{loss,out}$$

The total k-loss factor for IHX except k-loss due to contraction and expansion:

$$K_{IHX} = 2\rho_{IHX}\left(P_{1PDHX} - \Delta P_{SUMs}\right)\frac{A_{IHX}^2}{W_{IHX}|W_{IHX}|}$$

2.4.2 Hydraulics for Pipes (PIPE1S)

This subroutine solves the steady state flow equations for a pipe in the coolant loop. It is assumed that the diameter is constant, and the pipe wall is in thermal equilibrium with the coolant.

$$\Delta x_{node} = \Delta x_{pipe} / N_{1NODE}$$

$$sin_{SUM} = \sum_{i}^{N_{1NODE}-1} sin\phi_i$$

$$E_{OD} = (Roughness)/D_e$$

$$f = f(Re, E_{OD})$$

The total pressure drop in a pipe can be expressed in two different forms depend on locations. The pipe between IHX exit and pump inlet is not a real pipe and is used to minimize the modification of the SSC-L. Therefore, the pressure drop for the pipe between IHX exit and pump inlet includes the pressure drop due to gravitaion only. The density used in gravitational force calculation is assumed as the cold pool sodium density.

$$\Delta P_{drop}^{PIPE} = \rho_{cldp} \cdot g \cdot sin_{SUM} \cdot \Delta x_{node}$$ if pipe is between IHX exit and pump inlet

$$\Delta P_{drop}^{PIPE} = \left(f \frac{\Delta x_{pipe}}{D_e} + K \right) \frac{W|W|}{2\rho_{inlet} A^2} + \rho_{inlet} g \cdot sin_{SUM} \Delta x_{node} \qquad \text{else}$$

2.4.3 Pump (PUMP1S)

The pump rotating speed is determined by matching pump head and total hydraulic head.

The required pressure rise across pump is obtained from:

$$\Delta P_{pp} = \sum_{i}^{N_{1PIPE}} \Delta P_{drop_i}^{pipe} + P_{1PDRV} + P_{1PDCV}$$

where $\Delta P_{drop_i}^{pipe}$: pressure drop for pipe i

P_{1PDRV} : pressure drop from core inlet to IHX inlet

P_{1PDCV} : pressure drop in check valve

The pump head:

$$H_{pump} = \Delta P_{pp} / (\rho \cdot g)$$

$$h = H_{pump} / H_r$$

$$v = (W_{1REF} / \rho) / Q_r$$

$$\alpha = \Omega / \Omega_r$$

The α is found based on the value of h/v^2 from pump homologous curve using root finding scheme and pump rotational speed is obtained from:

$$\Omega = \alpha \cdot \Omega_r$$

2.4.4 Pressure Distribution of Pipes (PRES1S)

This subroutine set the pressure at the pipe end point.

$$P_{1OUT,1} = P_{1IN,1} - P_{DROP,1}$$

where $P_{1OUT,1}$: outlet pressure for pipe 1 in primary loop

$P_{1IN,1}$: inlet pressure for pipe 1 in primary loop (IHX inlet pressure)

$P_{DROP,1}$: pressure drop in pipe 1

For pipe 2 to N1PIPE, the $P_{1IN,i}$ is set to zero except the pipe after pump.

$$\begin{cases} P_{1IN,i} = \Delta P_{pump}^{rise} & \text{if } i = \text{pipe index for the pipe after pump} \\ P_{1IN,i} = 0 & \text{else} \end{cases}$$

Then, the pressure at a pipe inlet equals the sum of pressure at the previous pipe outlet and pressure drop due to any device (i.e., pump) between the pipes.

$$P_{1IN,i} = P_{1IN,i} + P_{1OUT,i-1} \qquad \text{for } i = 2, \quad N_{1PIPE}$$

$$P_{1IOUT,i} = P_{1IN,i} - P_{DROP,i} \qquad \text{for } i = 2, \quad N_{1PIPE}$$

2.4.5 Cold Pool Hydraulics (RES1S)

The sodium enthalpy in cold pool is assumed to the IHX exit enthalpy.

$$h_{cp} = h_{Xout}$$

The liquid level in cold pool is obtained from pressure difference between the cover gas pressure and the pump inlet pressure.

$$Z_{cp} = Z_{Pin} + \frac{P_{Pin} - P_{gas}}{\rho_{Pin} \cdot g}$$

Then, the cold pool sodium mass is obtained from the sodium level in cold pool by assuming that the cold pool can represented by two distinct regions with different cross-sectional area:

$$M_{cp} = \begin{cases} V_{b-pmp} + A_{cldp-c} \cdot Z_{cldp-c} + A_{ovf}(Z_{cp} - Z_{Xo}) & \text{if } Z_{cp} > Z_{Xo} \\ V_{b-pmp} + A_{cldp-c} \cdot (Z_{cp} - Z_{Pin}) & \text{if } Z_{cp} \le Z_{Xo} \end{cases}$$

3. TRANSIENT MODELS

The dynamic response of the primary coolant in a pool-type LMR, particularly the hot pool concept like KALIMER, can be quite different from response in the loop-type LMR. The difference arises primarily from the lack of direct piping connections between components in the hot and cold pools. Even through there are free surfaces in the reactor vessel and pump tank of loop-type designs, the direct piping connections permit the use of basically a single momentum equation to characterize the coolant dynamics in the primary loop, except in a transient initiated by pipe rupture or similar asymmetric initiator. In KALIMER, both hot and cold pools have free surfaces and there is direct mixing of the coolant with these open pools prior to entering the next component. At least two different flows would have to be modeled to characterize the coolant dynamics of the primary system. During steady-state the two flow rates can be obtained by a simple algebraic equation. During a transient, however, the flow from the pump to hot pool would respond to the pump head and losses in that circuit including losses in the core; the IHX flow would respond to the level difference between the two pools, as well as losses and gravity gains in the IHX. The gravity gain could be significant for low-flow conditions, particularly if the IHX gets overcooled due to a mismatch of primary and secondary flows. The flow chart for transient routine is in Fig. 3.1.

3.1. Flow Equations

Since the primary system of KALIMER has same number of pumps and IHXs, the first version of SSK-K has developed with constraint that the number of pumps has to be same as the number of IHXs. In SSC-K, the concept of flow paths (N_{path}) is introduced and each flow path includes one pump and one IHX.

3.1.1. Intact System

For an intact system, volume-averaged momentum equations can be written as follows:

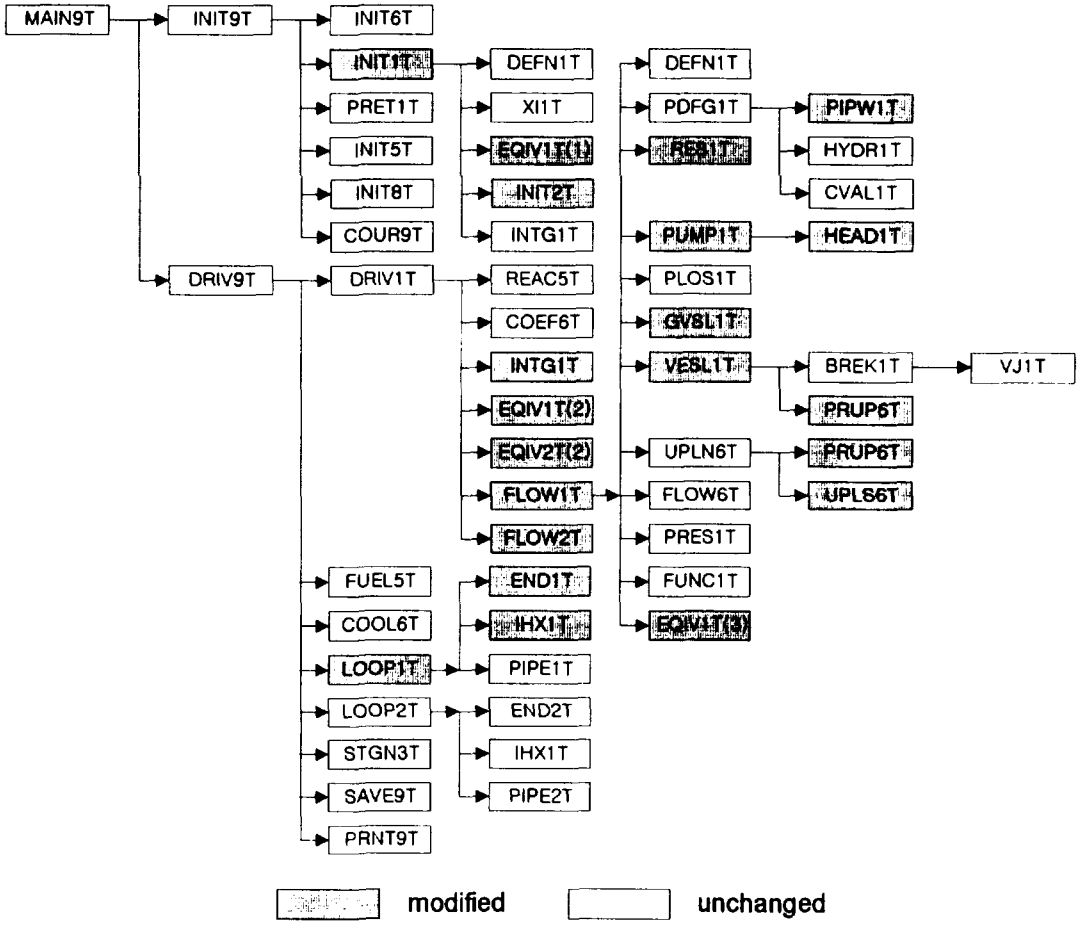

Fig. 3.1: Flowchart for Transient Calculation

Pump Flow

$$\frac{dW_p(k)}{dt}\sum_p \frac{L(k)}{A(k)} = P_{Po}(k) - P_{Rin} - \sum_p \Delta P_{f,g}(k), \qquad k = 1,\cdots, N_{path} \tag{3-1}$$

In above equation, the pump exit pressure, P_{Po}, is obtained from

$$P_{Po} = P_{Pin} + \rho_{Pin} g\, H \tag{3-2}$$

where H is the pump head, obtained from the pump characteristics.

IHX Flow

$$\frac{dW_{1X}(k)}{dt}\sum_X \frac{L(k)}{A(k)} = P_{Xin} - P_{Xo} - \sum_X \Delta P_{f,g}(k), \qquad k = 1,\cdots, N_{path} \tag{3-3}$$

The IHX inlet and exit pressures, P_{Xin} and P_{Xo}, are obtained from static balance as

$$P_{Xin} = P_{gas} + \rho_h g(Z_{HP} - Z_{Xin}) \tag{3-4}$$

$$P_{Xo} = P_{gas} + \rho_c g(Z_{CP} - Z_{Xo}) \tag{3-5}$$

The core inlet pressure, P_{Rin}, is obtained from a complicated algebraic equation and the derivation will be discussed later.

3.1.2. Damaged System

In KALIMER, the pipe rupture can only happen in pump discharge line to reactor core. For the broken path, Eq. (3-1) has to be modified to:

$$\frac{dW_p}{dt}\sum_{uob}\frac{L}{A} = P_{Po} - P_{bin} - \sum_{uob}\Delta P_{f,g} \tag{3-6}$$

An additional equation is needed to describe the flow downsteam of the break:

$$\frac{dW_{dob}}{dt}\sum_{dob}\frac{L}{A} = P_{bo} - P_{Rin} - \sum_{dob}\Delta P_{f,g} \tag{3-7}$$

The inlet and outlet pressures at break locatioon, P_{bin} and P_{bo}, respectively, are calculated by break model. The break model in SSC-K is same as that in SSC-L. The external pressure for the break, which is needed to compute these pressures, is obtained from static balance as

$$P_{ext} = P_{gas} + \rho_C g(Z_{CP} - Z_b) \tag{3-8}$$

This pressure acts as the back pressure opposing the flow out of the break. The value of this pressure is much larger than that for loop-type design, which is generally equal to atmospheric pressure until the sodium in guard vessel covers the break location. This will make the pipe break in pool-type designs less sever relative to loop-type designs.

3.2 Pump Suction Pressure

Fig. 3.1 shows a schematic of SSC-K Modeling for KALIMER. As you may be noticed, there is a pipe after IHX which does not exist in KALIMER. This pipe is included to minimize the modification of loop type version of SSC-K. This pipe is used to make the elevation of IHX exit same as the elevation of pump inlet. The pump surge tank model in loop-type version of SSC is used as a basis of the cold pool model in KALIMER. Pump surge tank in a loop-type LMR has similar characteristics with cold pool in pool-type LMR in many aspects. Both components include two distinct regions. In one region, the sodium is present in lower part while the second region is filled with noncondensable gas on the top of the sodium. The sodium levels in both components are changing with mass balance between IHX exit flow and pump inlet flow. However, some differences exist between two components. First, cover gas in pump surge tank is separated by cover gas in vessel while

cover gas in cold pool is in common with cover gas above hot pool. Second, enthalpy in pump surge tank is assumed to be same as enthalpy of IHX exit flow. This is a reasonable assumption for pump surge tank because of its small volume. However, it is not true in cold pool, which has relatively large sodium inventory. Therefore, energy equation is added in cold pool model to account the energy stored in sodium. And it is assumed that the entire pump inlet flow is from cold pool and no direct flow from IHX exit. The energy balance in cold pool will be discussed in later section.

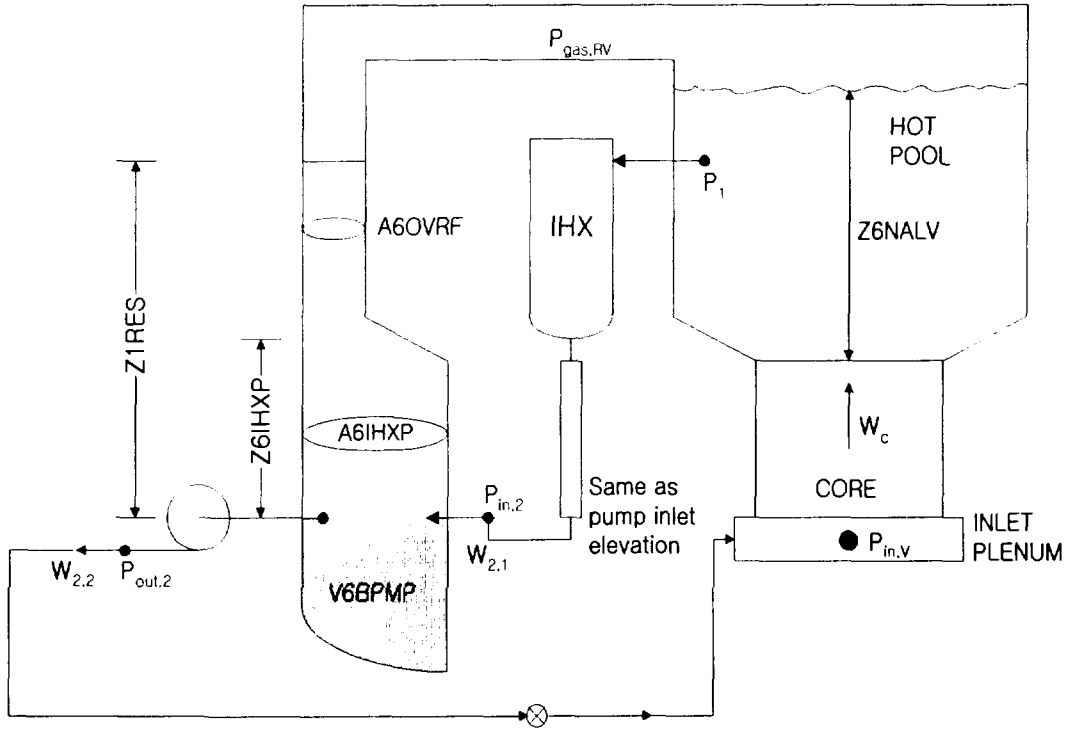

Fig. 3.2: Schematic of SSC-K Modeling for KALIMER

As seen in Fig. 3.2, a few variables are newly defined to model a cold pool and their descriptions are as follows:

- V6BPMP: Volume below pump inlet
- Z6IHXP: Elevation change from pump suction to IHX exit
- A6IHXP: Average flow area from pump suction to IHX exit
- A6OVRF: Average flow area for overflow path
- B6CLDP: Sodium mass of cold pool
- E6CLDP: Sodium average enthalpy of cold pool
- T6CLDP: Sodium average temperature of cold pool
- D6CLDP: Sodium average density of cold pool

The pump inlet pressure is obtained by adding cover gas pressure with elevation head of cold pool:

$$P_{Pin} = P_{gas} + \rho_c g(Z_{CP} - Z_{Pin}) \tag{3-9}$$

3.3 Liquid Levels in Pools

The liquid levels in cold and hot pools can be obtained by mass balance at each pool. The total flow through all the IHXs and all the pumps can be determined from:

$$W_{Xtot} = \sum_{k=1}^{N_{path}} W_X(k) \tag{3-10}$$

and

$$W_{Ptot} = \sum_{k=1}^{N_{path}} W_P(k) \tag{3-11}$$

Total sodium mass in cold pool is obtained by mass balance at the cold pool:

$$\frac{d}{dt}(\rho V)_{CP} = W_{Xtot} - W_{Ptot} + W_{ovf} + W_b \tag{3-12}$$

Note that the break flow, W_b, is zero for an intact system and the overflow from hot pool, W_{ovf}, is zero if the hot pool level is below the top of thermal liner. Then, the cold pool level can be obtained from the sodium mass in cold pool by assuming that the cold pool can represented by two distinct regions with different cross-sectional area:

$$(\rho V)_{CP} = \begin{cases} \rho_{cp}\left\{V_{bpmp} + A_{IHXP}\cdot Z_{IHXP} + A_{ovf}\cdot\left(Z_{cp} - Z_{IHXP}\right)\right\} \\ \qquad\qquad \text{if} \quad (\rho V)_{CP} > \rho_{cp}\cdot(V_{bpmp} + A_{IHXP}\cdot Z_{IHXP}) \\ \rho_{cp}\left\{V_{bpmp} + A_{IHXP}\cdot Z_{cp}\right\} \\ \qquad\qquad \text{if} \quad (\rho V)_{CP} \le \rho_{cp}\cdot(V_{bpmp} + A_{IHXP}\cdot Z_{IHXP}) \end{cases} \tag{3-13}$$

where V_{bpmp} : Cold pool volume below flow skirt

A_{IHXP} : Average cold pool cross-sectional area between flow skirt botton and IHX exit

Z_{IHXP} : Height from flow skirt botton to IHX exit

A_{ovf} : Average cold pool cross-sectional area above IHX exit

The time rate change of sodium mass in hot pool is obtained by mass balance at the hot pool:

$$A_{HP}\frac{d}{dt}(\rho Z)_{HP} = W_C - W_{Xtot} - W_{ovf} \tag{3-14}$$

Eq. (3-14) assumes that all the level changes likely to occur during the transient are confined to a constant cross-sectional area. When equations (3-12), (3-13) and (3-14) are solved simultaneously with the flow equations, the sodium levels for hot and cold pool during the transient can be obtained.

3.4 Reactor Internal Pressure

The reactor internal pressure, P_{Rin}, for both an intact and a damaged system is

derived in the following section.

3.4.1 Intact system

Mass conservation at core inlet yields

$$W_C = \sum_{k=1}^{N_{path}} W_P(k) \tag{3-15}$$

Differentiating both sides with time yields

$$\frac{dW_C}{dt} = \sum_{k=1}^{N_{path}} \frac{dW_P(k)}{dt} \tag{3-16}$$

The core flow can be expressed in terms of channel flows as

$$W_C = \sum_{j=1}^{N_{ch}} W_j \tag{3-17}$$

where N_{ch} represents the number of channels simulated in the core. Differentiating both sides with time gives

$$\frac{dW_C}{dt} = \sum_{j=1}^{N_{ch}} \frac{dW_j}{dt} \tag{3-18}$$

Time rate of core flow change for each channel can be written from momentum balance

$$\frac{dW_j}{dt}\left(\sum \frac{L}{A}\right)_j = P_{Rin} - P_{Ro} - \left(\sum \Delta P_{f,g}\right)_j \tag{3-19}$$

$$P_{Ro} = P_g + \rho_H g(Z_{HP} - Z_{Ro}) . \tag{3-20}$$

Combining Eqs. (3-16), (3-18) and (3-19) gives

$$\sum_{k=1}^{N_{path}} \frac{dW_p(k)}{dt} = \sum_j \left\{ \frac{P_{Rin} - P_{Ro} - \left(\sum \Delta P_{f,g}\right)_j}{\left(\sum L/A\right)_j} \right\} \tag{3-21}$$

Substituting Eq. (3-1) into the left hand side of Eq. (3-21) gives

$$\sum_{k=1}^{N_{path}} \left[\frac{P_{Po}(k) - P_{Rin} - \sum_p \Delta P_{f,g}(k)}{\sum_p \frac{L(k)}{A(k)}} \right] = \sum_j \left\{ \frac{P_{Rin} - P_{Ro} - \left(\sum \Delta P_{f,g}\right)_j}{\left(\sum L/A\right)_j} \right\} \tag{3-22}$$

Simplifying Eq. (3-22) yields the core inlet pressure as

$$P_{Rin} = \frac{A+B}{C+D} \tag{3-23}$$

where

$$A = \sum_j \left\{ \frac{P_{Ro} + \left(\sum \Delta P_{f,g}\right)_j}{\left(\sum L/A\right)_j} \right\} \tag{3-24}$$

$$B = \sum_{k=1}^{N_{path}} \left[\frac{P_{Po}(k) - \sum_p \Delta P_{f,g}(k)}{\sum_p \{L(k)/A(k)\}} \right] \tag{3-25}$$

$$C = \sum_j \left\{ \frac{1}{\left(\sum L/A\right)_j} \right\} \tag{3-26}$$

$$D = \sum_{k=1}^{N_{path}} \left[\frac{1}{\sum_{p} \{L(k)/A(k)\}} \right] \tag{3-27}$$

3.4.2 Damaged System

In case of a pipe rupture in one of the pump discharge lines, mass conservation at core inlet has to account for the downstream flow of break to core.

$$W_C = \sum_{\substack{k=1 \\ \neq brk}}^{N_{path}} W_P(k) + W_{dob} \tag{3-28}$$

Differentiating both sides with time yields

$$\frac{dW_C}{dt} = \sum_{\substack{k=1 \\ \neq brk}}^{N_{path}} \frac{dW_P(k)}{dt} + \frac{dW_{dob}}{dt} \tag{3-29}$$

Combining Eqs. (3-19 and (3-29) gives

$$\sum_{\substack{k=1 \\ \neq brk}}^{N_{path}} \frac{dW_P(k)}{dt} + \frac{dW_{dob}}{dt} = \sum_{j} \left\{ \frac{P_{Rin} - P_{Ro} - \left(\sum \Delta P_{f.g}\right)_j}{\left(\sum L/A\right)_j} \right\} \tag{3-30}$$

Substituting Eqs. (3-1) and (3-7) into the left hand side of Eq. (3-30) gives

$$\sum_{\substack{k=1 \\ \neq brk}}^{N_{path}} \left[\frac{P_{Po}(k) - P_{Rin} - \sum_{p} \Delta P_{f.g}(k)}{\sum_{p} \frac{L(k)}{A(k)}} \right] + \frac{P_{bo}(k) - P_{Rin} - \sum_{dob} \Delta P_{f.g}(k)}{\sum_{dob} \frac{L(k)}{A(k)}} = \sum_{j} \left\{ \frac{P_{Rin} - P_{Ro} - \left(\sum \Delta P_{f.g}\right)_j}{\left(\sum L/A\right)_j} \right\} \tag{3-31}$$

Simplifying Eq. (3-31) yields the core inlet pressure as

$$P_{Rin} = \frac{A+B+C}{D+E+F} \tag{3-32}$$

where

$$A = \sum_{j} \left\{ \frac{P_{Ro} + \left(\sum \Delta P_{f,g}\right)_j}{\left(\sum L/A\right)_j} \right\} \tag{3-33}$$

$$B = \sum_{\substack{k=1 \\ \neq brk}}^{N_{path}} \left[\frac{P_{Po}(k) - \sum_{p} \Delta P_{f,g}(k)}{\sum_{p} \{L(k)/A(k)\}} \right] \tag{3-34}$$

$$C = \frac{P_{bo}(k) - \sum_{dob} \Delta P_{f,g}(k)}{\sum_{dob} \{L(k)/A(k)\}} \tag{3-35}$$

$$D = \sum_{j} \left\{ \frac{1}{\left(\sum L/A\right)_j} \right\} \tag{3-36}$$

$$E = \sum_{\substack{k=1 \\ \neq brk}}^{N_{path}} \left[\frac{1}{\sum_{p} \{L(k)/A(k)\}} \right] \tag{3-37}$$

$$F = \frac{1}{\sum_{dob} \{L(k)/A(k)\}} \tag{3-38}$$

3.5 Energy Balance in Hot Pool

Thermal stratification can occur in the hot pool region if the entering coolant is colder than the existing hot pool coolant and the flow momentum is not large enough to overcome the negative buoyancy force. Since the fluid of hot pool enters IHXs, the temperature distribution of hot pool can alter the overall system response. Hence, it is necessary to predict the pool coolant temperature distribution with sufficient accuracy to determine the inlet temperature conditions for the IHXs and its contribution to the net buoyancy head.

During a normal reactor scram, the heat generation is reduced almost instantaneously while the coolant flow rate follows the pump coastdown. This mismatch between power and flow results in a situation where the core flow entering the hot pool is at a lower temperature than the temperature of the bulk pool sodium. This temperature difference leads to stratification when the decaying coolant momentum is insufficient.

The stratification of the core flow in the hot pool is represented by a two-zone model based on the model for mixing in the upper plenum of loop-type LMRs in SSC-L (Fig. 3.3). The hot pool is divided into two perfectly mixing zones determined by the maximum penetration distance of the core flow. This penetration distance is a function of the Froude number of the average core exit flow. The temperature of each zone is computed from energy balance considerations. The temperature of the upper portion, T_A, will be relatively unchanged; in the lower region, however, T_B will be changed and somewhat between the core exit temperature and the temperature of upper zone due to active mixing with core exit flow as well as heat transfer with the upper zone. The temperature of upper zone is mainly affected by interfacial heat transfer. Full penetration is assumed for flow with positive buoyancy.

The two-zone model in SSC-L has some difficulties to maintain the mass and energy conservation in the hot pool because it does not account for the mass and energy change due to the variation of penetration height. Therefore, the following equations for energy balance is adopted in SSC-K.

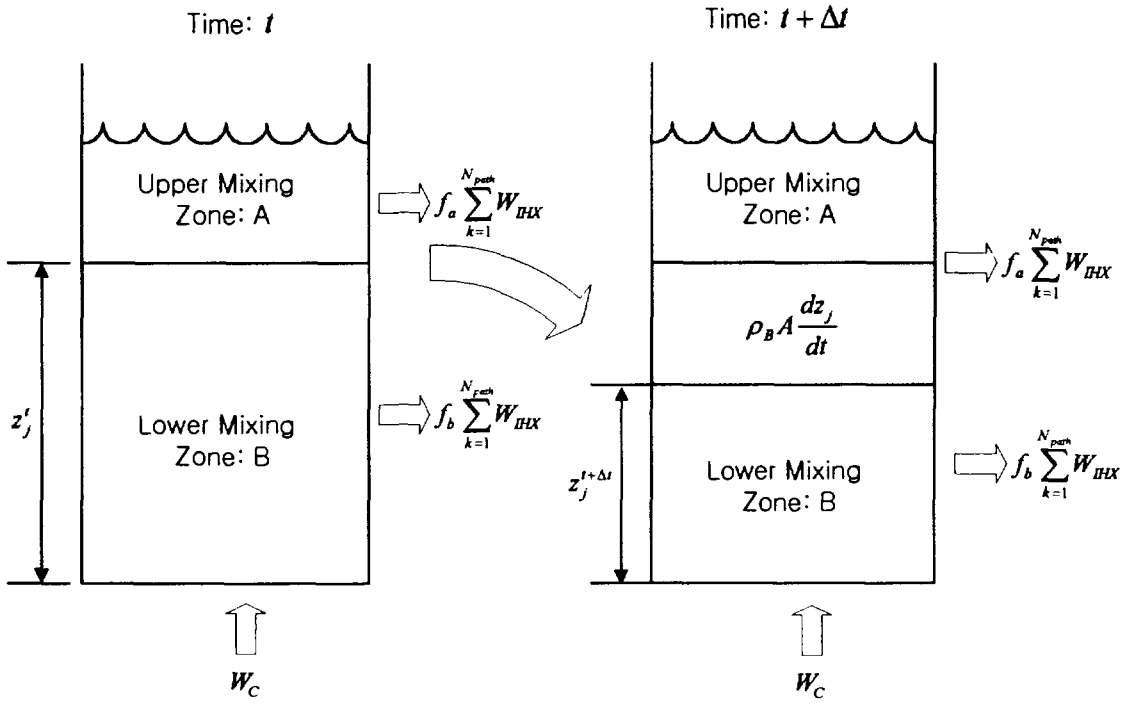

Fig. 3.3: Two mixing zone model for hot pool

The non-conservative form of energy balance equations which determine the various temperatures in the hot pool are given below:

3.5.1. Lower mixing zone B:

3.5.1.1 Case 1: $\frac{dz_j}{dt} > 0$

Mass conservation

$$\frac{d}{dt}(\rho V)_B = \frac{dz_j}{dt}\rho_A A + W_C - f_B \sum_{k=1}^{Npath} W_{IHX}(k) \qquad (3\text{-}39)$$

Energy Conservation

$$\frac{d}{dt}(\rho EV)_B = \frac{dz_j}{dt}\rho_A AE_A + W_C E_{Ro} - f_B \sum_{k=1}^{Npath} W_{IHX} E_B - UA_{bm2}(T_B - T_{m2}) - UA_{hm1}(1-f)(T_B - T_{m1}) - hA_{ba}(T_B - T_A) \quad (3\text{-}40)$$

Expand derivative in energy equation for total mass and enthalpy:

$$(\rho V)_B \frac{dE_B}{dt} + E_B \frac{d}{dt}(\rho V)_B = \frac{dz_j}{dt}\rho_A AE_A + W_C E_{Ro} - f_B \sum_{k=1}^{Npath} W_{IHX} E_B - UA_{bm2}(T_B - T_{m2}) - UA_{hm1}(1-f)(T_B - T_{m1}) - hA_{ba}(T_B - T_A) \quad (3\text{-}41)$$

Combine above equation with mass conservation equation and rearrange the nonconservative form of energy equation:

$$\rho_B V_B \frac{dE_B}{dt} = \frac{dz_j}{dt}\rho_A A(E_A - E_B) + W_C(E_{Ro} - E_B) - UA_{bm2}(T_B - T_{m2}) - UA_{hm1}(1-f)(T_B - T_{m1}) - hA_{ba}(T_B - T_A) \quad (3\text{-}42)$$

3.5.1.2 Case 2: $\frac{dz_j}{dt} < 0$

Mass conservation

$$\frac{d}{dt}(\rho V)_B = \frac{dz_j}{dt}\rho_B A + W_C - f_B \sum_{k=1}^{Npath} W_{IHX}(k) \quad (3\text{-}43)$$

Energy Conservation

$$\frac{d}{dt}(\rho EV)_B = \frac{dz_j}{dt}\rho_B A E_B + W_C E_{Ro} - f_B \sum_{k=1}^{Npath} W_{IHX} E_B - UA_{bm2}(T_B - T_{m2}) - UA_{hm1}(1-f)(T_B - T_{m1}) - hA_{ba}(T_B - T_A) \quad (3\text{-}44)$$

Expand derivative in energy equation for total mass and enthalpy:

$$(\rho V)_B \frac{dE_B}{dt} + E_B \frac{d}{dt}(\rho V)_B = \frac{dz_j}{dt}\rho_B A E_B + W_C E_{Ro} - f_B \sum_{k=1}^{Npath} W_{IHX} E_B - UA_{bm2}(T_B - T_{m2}) - UA_{hm1}(1-f)(T_B - T_{m1}) - hA_{ba}(T_B - T_A) \quad (3\text{-}45)$$

Combine above equation with mass conservation equation and rearrange the nonconservative form of energy equation:

$$\rho_B V_B \frac{dE_B}{dt} = W_C(E_{Ro} - E_B) - UA_{bm2}(T_B - T_{m2}) - UA_{hm1}(1-f)(T_B - T_{m1}) - hA_{ba}(T_B - T_A) \quad (3\text{-}46)$$

3.5.2. Upper mixing zone A:

3.5.2.1. Case 1: $\frac{dz_j}{dt} > 0$

Mass conservation

$$\frac{d}{dt}(\rho V)_A = -\frac{dz_j}{dt}\rho_A A - f_A \sum_{k=1}^{Npath} W_{IHX}(k) - W_{orf} \quad (3\text{-}47)$$

Energy Conservation

$$\frac{d}{dt}(\rho EV)_A = -\frac{dz_j}{dt}\rho_A AE_A - f_A\sum_{k=1}^{Npath} W_{IHX}E_A - W_{orf}E_A$$
$$-UA_{am2}(T_A - T_{m2}) - UA_{hm1}f(T_A - T_{m1}) - UA_{hg}(T_A - T_g) + hA_{ba}(T_B - T_A) \quad (3\text{-}48)$$

Expand derivative in energy equation for total mass and enthalpy:

$$(\rho V)_A\frac{dE_A}{dt} + E_A\frac{d}{dt}(\rho V)_A = -\frac{dz_j}{dt}\rho_A AE_A - f_A\sum_{k=1}^{Npath} W_{IHX}E_A - W_{orf}E_A$$
$$-UA_{am2}(T_A - T_{m2}) - UA_{hm1}f(T_A - T_{m1}) - UA_{hg}(T_A - T_g) + hA_{ba}(T_B - T_A) \quad (3\text{-}49)$$

Combine above equation with mass conservation equation and rearrange the nonconservative form of energy equation:

$$(\rho V)_A\frac{dE_A}{dt} = -UA_{am2}(T_A - T_{m2}) - UA_{hm1}f(T_A - T_{m1})$$
$$-UA_{hg}(T_A - T_g) + hA_{ba}(T_B - T_A) \quad (3\text{-}50)$$

3.5.2.2. Case 2: $\frac{dz_j}{dt} < 0$

Mass conservation

$$\frac{d}{dt}(\rho V)_A = -\frac{dz_j}{dt}\rho_B A - f_A\sum_{k=1}^{Npath} W_{IHX}(k) - W_{orf} \quad (3\text{-}51)$$

Energy Conservation

$$\frac{d}{dt}(\rho EV)_A = -\frac{dz_j}{dt}\rho_B AE_B - f_A\sum_{k=1}^{Npath} W_{IHX}E_A - W_{orf}E_A$$
$$-UA_{am2}(T_A - T_{m2}) - UA_{hm1}f(T_A - T_{m1}) - UA_{hg}(T_A - T_g) + hA_{ba}(T_B - T_A) \quad (3\text{-}52)$$

Expand derivative in energy equation for total mass and enthalpy:

$$(\rho V)_A \frac{dE_A}{dt} + E_A \frac{d}{dt}(\rho V)_A = -\frac{dz_j}{dt}\rho_B A E_B - f_A \sum_{k=1}^{Npath} W_{IHX} E_A - W_{orf} E_A \\ -UA_{am2}(T_A - T_{m2}) - UA_{hm1} f(T_A - T_{m1}) - UA_{hg}(T_A - T_g) + hA_{ba}(T_B - T_A) \quad (3\text{-}53)$$

Combine above equation with mass conservation equation and rearrange the nonconservative form of energy equation:

$$(\rho V)_A \frac{dE_A}{dt} = -\frac{dz_j}{dt}\rho_B A(E_B - E_A) - UA_{am2}(T_A - T_{m2}) \\ -UA_{hm1} f(T_A - T_{m1}) - UA_{hg}(T_A - T_g) + hA_{ba}(T_B - T_A) \quad (3\text{-}54)$$

3.5.3. Other temperatures in hot pool

Upper internal structure (metal m1):

$$M_{m1} C_{m1} \frac{dT_{m1}}{dt} = UA_{hm1}[f T_A + (1-f)T_B - T_{m1}] - UA_{gm1}(T_{m1} - T_g) \quad (3\text{-}55)$$

Barrier (metal m2):

$$M_{m2} C_{m2} \frac{dT_{m2}}{dt} = UA_{hm2}\left[\frac{A_{am2} T_A + A_{bm2} T_B}{A_{hm2}} - T_{m2}\right] - UA_{cm2}(T_{m2} - T_{CP}) \quad (3\text{-}56)$$

U_{hm2} is not very sensitive to changes in sodium temperature, and so this equation is derived assuming $U_{bm2} = U_{am2}$.

Roof (metal m3):

$$M_{m3}C_{m3}\frac{dT_{m3}}{dt} = UA_{gm3}(T_g - T_{m3}) \tag{3-57}$$

The heat transfer from the roof to the ambient has been neglected.

Cover gas:

$$\begin{aligned} M_g C_g \frac{dT_g}{dt} = {} & UA_{hg}(T_A - T_g) - UA_{cg}(T_g - T_{CP}) \\ & + UA_{gm1}(T_{m1} - T_g) - UA_{gm3}(T_g - T_{m3}) \end{aligned} \tag{3-58}$$

The auxiliary equations required by the above governing equations are

$$A_{ba} = \pi D^2 / 4 \tag{3-59}$$

$$f = 1 - z_j(t) / (Z_{HP} - Z_{Ro}) \tag{3-60}$$

3.6 Energy Balance in Cold Pool

Currently, perfect mixing of the IHX flow with the cold pool sodium is assumed. Energy balance equation for cold pool is derived as:

Mass Conservation

$$\frac{d}{dt}(\rho V)_{cp} = \sum_{N_{path}} W_{IHX} - \sum_{N_{path}} W_{pmp} + W_{ovf} + \sum_{N_{path}} W_{brk} \tag{3-61}$$

Energy Conservation

$$\frac{d}{dt}(\rho h V)_{cp} = \sum_{N_{path}} W_{IHX} h_{IHX} - \sum_{N_{path}} W_{pmp} h_{cp} + W_{ovf} h_{hp} + \sum_{N_{path}} W_{brk} h_{brk} \tag{3-62}$$

Expand derivative in energy equation for total mass and enthalpy:

$$(\rho V)_{cp}\frac{dh_{cp}}{dt}+h_{cp}\frac{d}{dt}(\rho V)_{cp}=\sum_{N_{path}}W_{IHX}h_{IHX} - h_{cp}\sum_{N_{path}}W_{pmp}+W_{ovf}h_{hp}+\sum_{N_{path}}W_{brk}h_{brk} \tag{3-63}$$

Combine above equation with mass conservation equation:

$$(\rho V)_{cp}\frac{dh_{cp}}{dt}+h_{cp}\left(\sum_{N_{path}}W_{IHX}-\sum_{N_{path}}W_{pmp}+W_{ovf}\right) = \sum_{N_{path}}W_{IHX}h_{IHX}-h_{cp}\sum_{N_{path}}W_{pmp}+W_{ovf}h_{hp}+\sum_{N_{path}}W_{brk}h_{brk} \tag{3-64}$$

Rearrange the nonconservative form of energy equation:

$$(\rho V)_{cp}\frac{dh_{cp}}{dt}=\sum_{N_{path}}W_{IHX}h_{IHX}-h_{cp}\sum_{N_{path}}W_{IHX} +W_{ovf}h_{hp}-W_{ovf}h_{cp}+\sum_{N_{path}}W_{brk}h_{brk}-h_{cp}\sum_{N_{path}}W_{brk} \tag{3-65}$$

Above equation can be expressed into two different equations depend on the direction of break flow.

$$(\rho V)_{cp}\frac{dh_{cp}}{dt}= \begin{cases} \sum_{N_{path}}W_{IHX}h_{IHX}-h_{cp}\sum_{N_{path}}W_{IHX}+W_{ovf}(h_{hp}-h_{cp}) \\ \qquad +\sum_{N_{path}}W_{brk}h_{brk}-h_{cp}\sum_{N_{path}}W_{brk} & \text{if } W_{brk}>0 \\ \sum_{N_{path}}W_{IHX}h_{IHX}-h_{cp}\sum_{N_{path}}W_{IHX}+W_{ovf}(h_{hp}-h_{cp}) & \text{if } W_{brk}\le 0 \end{cases} \tag{3-66}$$

Discretize above equation in time:

$$h_{cp}^{t+\Delta t} - h_{cp}^{t} =$$

$$\begin{cases} \dfrac{\Delta t}{(\rho V)_{cp}} \left[\sum_{N_{path}} W_{IHX} h_{IHX} - h_{cp}^{t+\Delta t} \sum_{N_{path}} W_{IHX} + W_{ovf} h_{hp} \right. \\ \qquad \left. - W_{ovf} h_{cp}^{t+\Delta t} + \sum_{N_{path}} W_{brk} h_{brk} - h_{cp}^{t+\Delta t} \sum_{N_{path}} W_{brk} \right] & \text{if } W_{brk} > 0 \\ \dfrac{\Delta t}{(\rho V)_{cp}} \left[\sum_{N_{path}} W_{IHX} h_{IHX} - h_{cp}^{t+\Delta t} \sum_{N_{path}} W_{IHX} \right. \\ \qquad \left. + W_{ovf} h_{hp} - W_{ovf} h_{cp}^{t+\Delta t} \right] & \text{if } W_{brk} \le 0 \end{cases} \tag{3-67}$$

$$\begin{cases} h_{cp}^{t+\Delta t} \left\{ 1 + \dfrac{\Delta t}{(\rho V)_{cp}} \left(\sum_{N_{path}} W_{IHX} + W_{ovf} + \sum_{N_{path}} W_{brk} \right) \right\} \\ \quad = h_{cp}^{t} + \dfrac{\Delta t}{(\rho V)_{cp}} \left\{ \sum_{N_{path}} W_{IHX} h_{IHX} + W_{ovf} h_{hp} + \sum_{N_{path}} W_{brk} h_{brk} \right\} & \text{if } W_{brk} > 0 \\ h_{cp}^{t+\Delta t} \left\{ 1 + \dfrac{\Delta t}{(\rho V)_{cp}} \left(\sum_{N_{path}} W_{IHX} + W_{ovf} \right) \right\} \\ \quad = h_{cp}^{t} + \dfrac{\Delta t}{(\rho V)_{cp}} \left\{ \sum_{N_{path}} W_{IHX} h_{IHX} + W_{ovf} h_{hp} \right\} & \text{if } W_{brk} \le 0 \end{cases} \tag{3-68}$$

Solve for $h_{cp}^{t+\Delta t}$:

$$\begin{cases} h_{cp}^{t+\Delta t} = \dfrac{h_{cp}^{t} + \dfrac{\Delta t}{(\rho V)_{cp}}\left\{\sum_{N_{path}} W_{IHX} h_{IHX} + W_{ovf} h_{hp} + \sum_{N_{path}} W_{brk} h_{brk}\right\}}{1 + \dfrac{\Delta t}{(\rho V)_{cp}}\left(\sum_{N_{path}} W_{IHX} + W_{ovf} + \sum_{N_{path}} W_{brk}\right)} & if\ W_{brk} > 0 \\ h_{cp}^{t+\Delta t} = \dfrac{h_{cp}^{t} + \dfrac{\Delta t}{(\rho V)_{cp}}\left\{\sum_{N_{path}} W_{IHX} h_{IHX} + W_{ovf} h_{hp}\right\}}{1 + \dfrac{\Delta t}{(\rho V)_{cp}}\left(\sum_{N_{path}} W_{IHX} + W_{ovf}\right)} & if\ W_{brk} \le 0 \end{cases} \tag{3-69}$$

Lower structures (metal m4):

$$(MC)_{m4}\frac{dT_{m4}}{dt} = UA_{cm4}(T_{cp} - T_{m4}) \tag{3-70}$$

It should be noted that the heat transfer between structures and cold pool sodium is ignored in current version of SSC-K. The above equation will be adopted in later version.

4. Model Verifications

Test runs were made using SSC-K for the qualitative verification of the simulation capability of the pool version of SSC-K. Because the simulations were performed to investigate that the specific features for pool-type reactor is modeled as intended, the input utilized in these tests was not based upon a reference plant. Therefore, the analysis for verification is not focused on the values from the simulations, but the trends of the results.

4.1 Null Transient Calculation

To illustrate the steady-state calculation capability of SSC-K, the null transient calculation has been made for a full power operation condition of KALIMER. The null transient has been terminated after 2000 seconds. The results for this simulation are summarized in Table 4-1. The maximum change during 2000 seconds transient occurs in core power calculation with the range of ~1.2 % and all the remaining system parameters changes within ~0.5 % of their initial values. However, the computed values for the major parameters are stable enough and satisfies the standard for nuclear power plant simulators for use in operator training, ANSI/ANS-3.5-1979, which requests not to vary by more than 2% of the initial values during a continuous 60 minute period of operation.

Table 4-1: Major Parameters for Nominal Operating Condition

Descriptions	KALIMER	SSC-K Predictions		
		0 s	2000 s	% change
Core power, MWt	392.2	392.2	387.5	1.2
Primary Heat Transport System				
Primary flow rate, kg/s	2143.1	2143.10	2143.02	0.0
Core inlet temperature, °C	386.2	386.2	386.2	0.0

Core outlet temperature, °C	530.0	530.42	529.82	0.11
IHX inlet temperature, °C		530.42	529.82	0.11
IHX outlet temperature, °C		386.2	387.36	0.30
Max. fuel temerature[+], °C		593.71	592.43	0.21
Cover gas pressure, Pa	10133	10133	10125	0.08
Cover gas temperature, °C		513.61	513.39	0.04
Cold pool level, m	12.52	12.52	12.52	0.0
Hot pool level, m	15.92	15.92	15.92	0.0
Pump head, m	66.07	66.07	66.07	0.0
Intermediate Heat Transport System				
Intermediate flow, kg/s	1803.6	1794.47	1794.58	0.01
IHX inlet temperature, °C	339.7	339.69	340.31	0.18
IHX outlet temperature, °C	511.0	511.13	510.65	0.09
Reactivities				
Sodium reactivity, ¢		0.0	-0.00960685	
Doppler reactivity, ¢		0.0	0.00719491	

[+] fuel channel 1, 8[th] axial slice

4.2 Transient Simulations

4.2.1 Unprotected Loss of Heat Sink (ULOHS)

This event is assumed that the sodium in intermediate loop is dumped into the intermediate heat transport system dump tank to mitigate a sodium-water reaction, so that all heat generated is retained in the primary system. The primary pumps are assumed to operate normally, and the plant protection system is assumed not to scram the reactor. In order to simulate this event using SSC-K, the heat transfer coefficient between primary and

secondary systems was set to zero at 0 s.

The two cases of simulations have been performed to illustrate the cold pool effect during ULOHS accident. In first case, the small volume of cold pool is used to minimize the effect of cold pool. The second case is performed for larger volume of cold pool to examine the pool effect. As shown in Figs. 4.1 and 4.2, the sudden decrease of the heat transfer coefficient of IHX raises the cold pool sodium temperature slowly to the hot pool sodium temperature. Because of the small cold pool volume in the first test run, the cold pool sodium temperature changes more rapidly than the larger cold volume case. Figures 4.3 and 4.4 shows the sodium levels for hot and cold pools. In case 2, both hot and cold pool sodium levels increase while the levels in the case with smaller cold pool volume are stabilized. The main reason is that the less negative reactivity is inserted in case 2 due to lower cold pool temperature (Figs. 4.5 ~ 4.6).

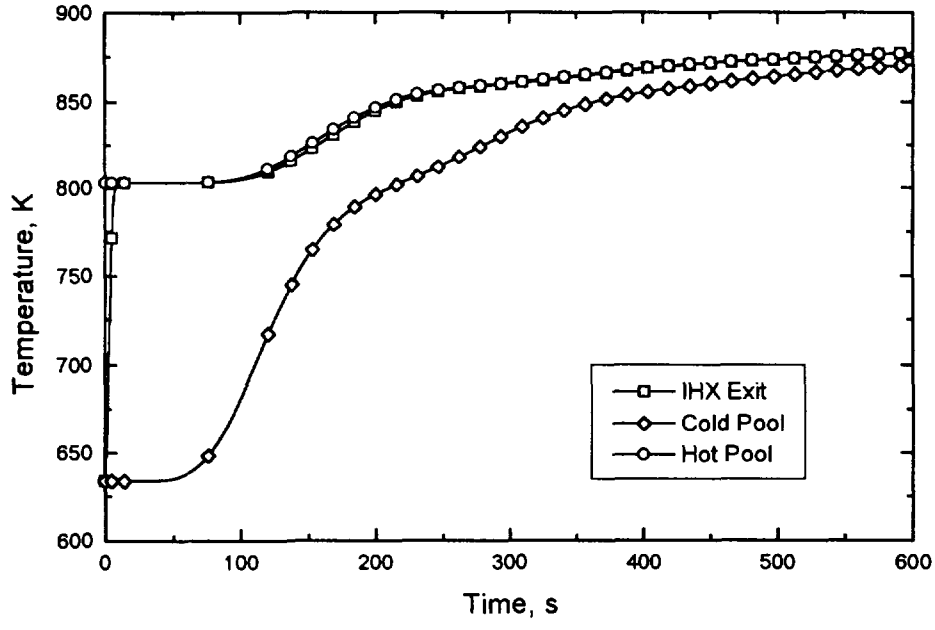

Fig. 4.1: Temperature for case 1
(V6BPMP: 0.1 m^3, A6IHXP: 0.2 m^2, A6OVFR: 0.1m^2)

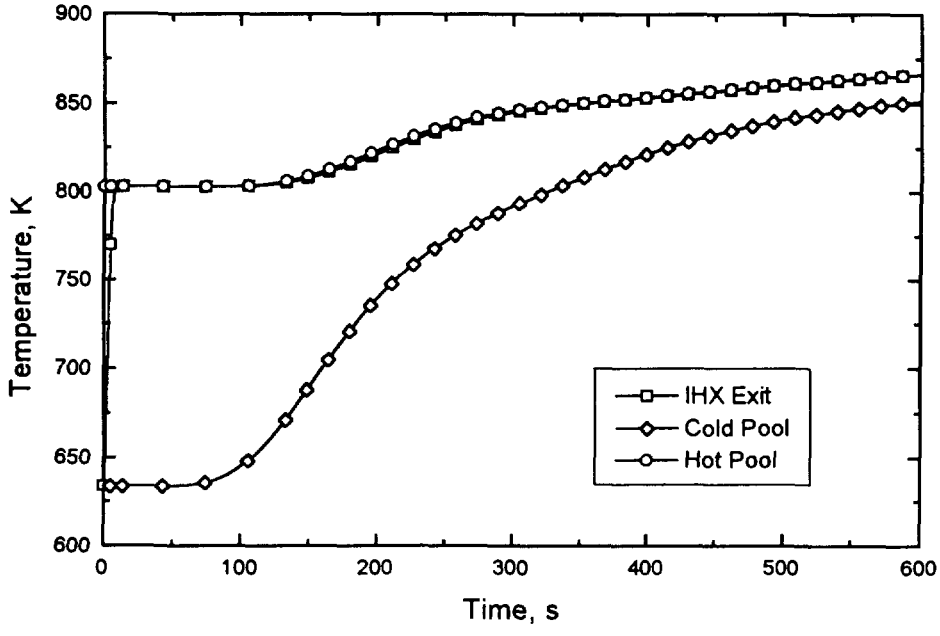

Fig. 4.2: Temperature for case 2
(V6BPMP: 100m^3, A6IHXP: 20m^2, A6OVRF: 1m^2)

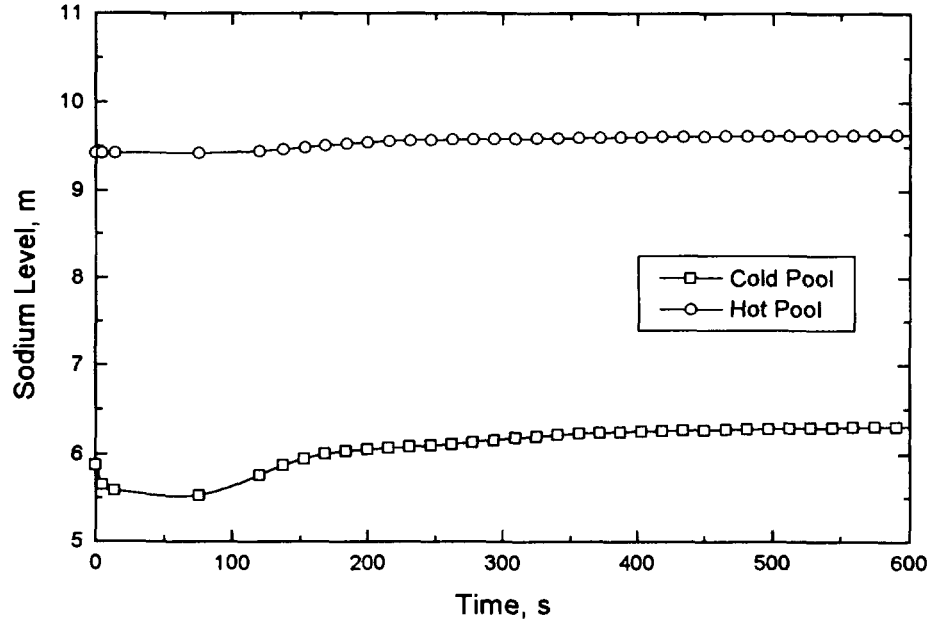

Fig. 4.3: Sodium levels for case 1

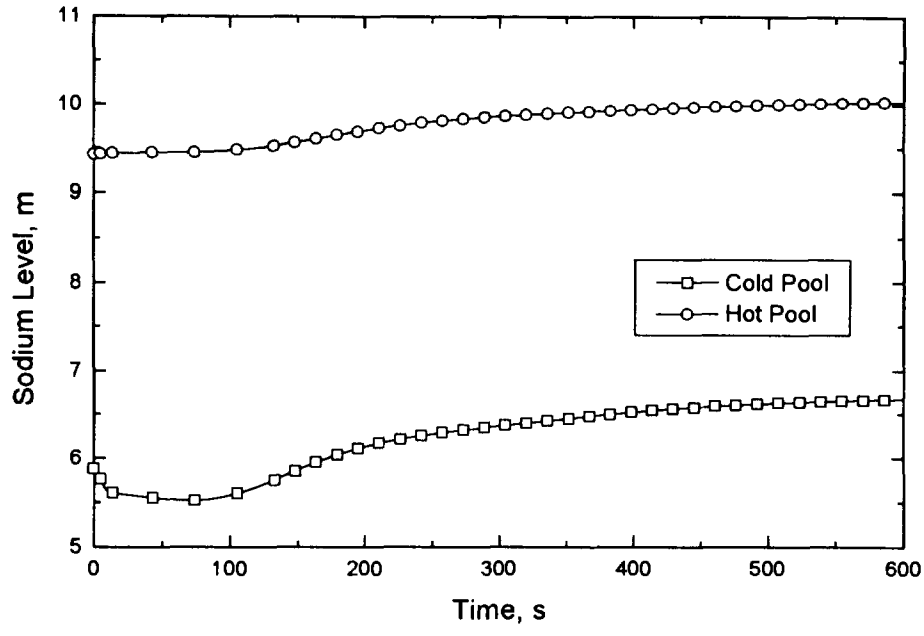

Fig. 4.4: Sodium levels for case 2

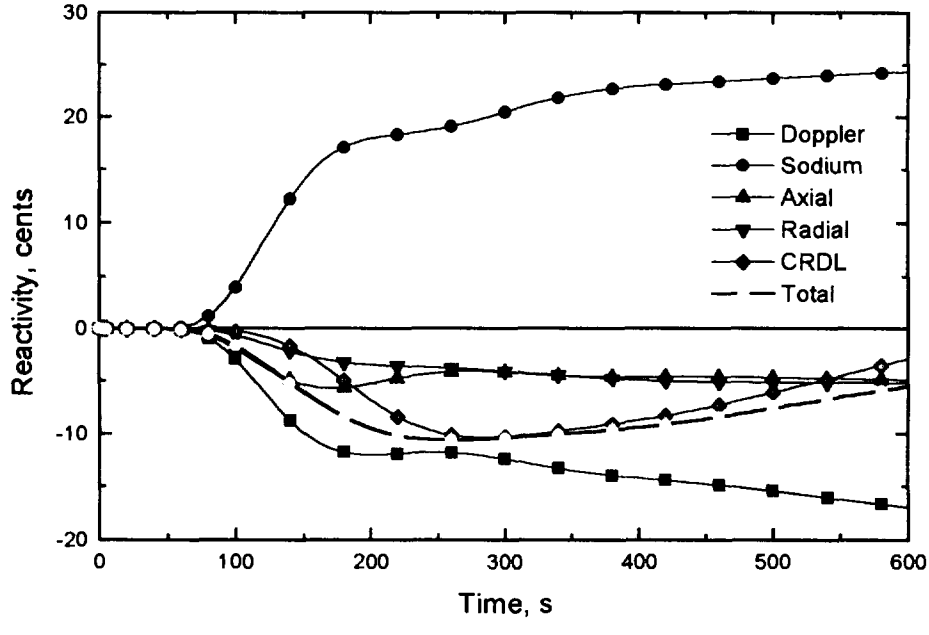

Fig. 4.5: Reactivity for case 1

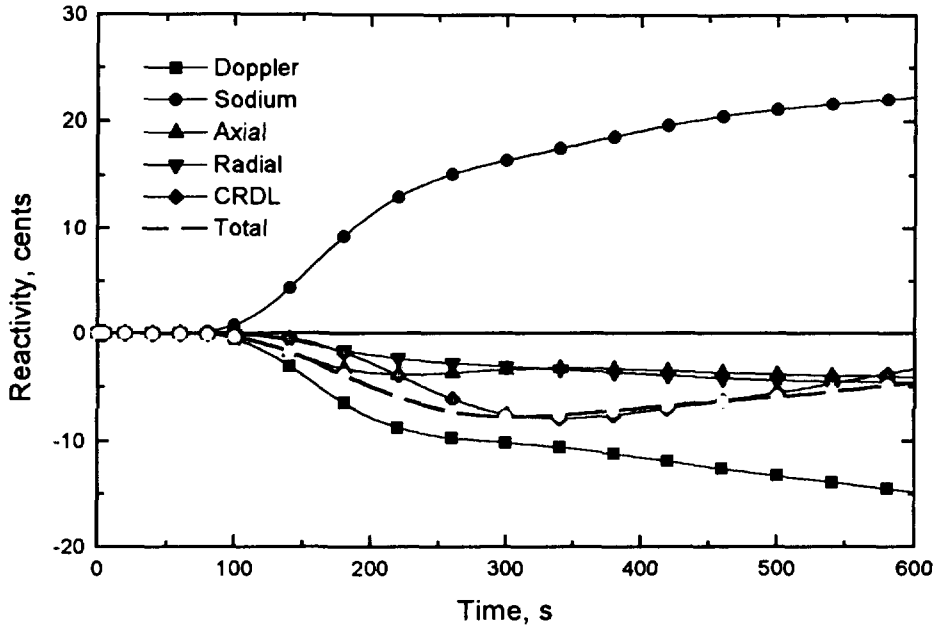

Fig. 4.6: Reactivity for case 2

4.2.2 Overflow Simulation

The liquid in the hot pool can be flooded into cold pool and forms the natural circulation flow path in some transients. During the loss of heat sink transients, this will provided as a major heat rejection mechanism with the passive decay heat removel system.

The transient was initiated by setting the heat transfer coefficient between primary and secondary systems to zero at 0 s. The primary pumps are assumed to operate normally, and the plant protection system is assumed not to scram the reactor. The height of the thermal barrier between hot and cold pools has been lowered to make easy to flood. In this test run, the passive decay heat removal system is not included.

Figure 4.7 shows the reactivity versus time during the transient. All the reactivity coefficients except sodium reactivity become negative due to temperature increases of sodium and fuel rod. Because there is no heat removal in IHX, the IHX exit sodium temperature immediately becomes to hot pool sodium temperature and cold pool sodium

temperature increases slowly due to large sodium inventory (Fig. 4.8). At ~200 s, hot pool sodium is flooded to cold pool and cold pool sodium level increases rapidly (Fig. 4.9). Figure 4.10 shows the flow rates for various flow paths. The pump flow is almost constant because pump are operated normally throughout the transient. But IHX flow starts to decrease as soon as the overflow from hot pool to cold pool starts.

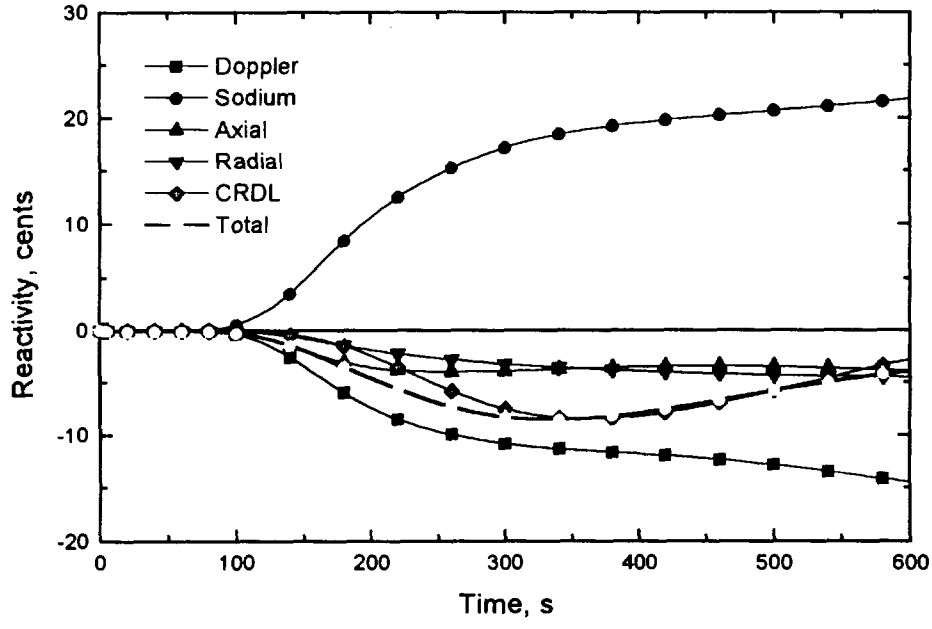

Fig. 4.7: Reactivity

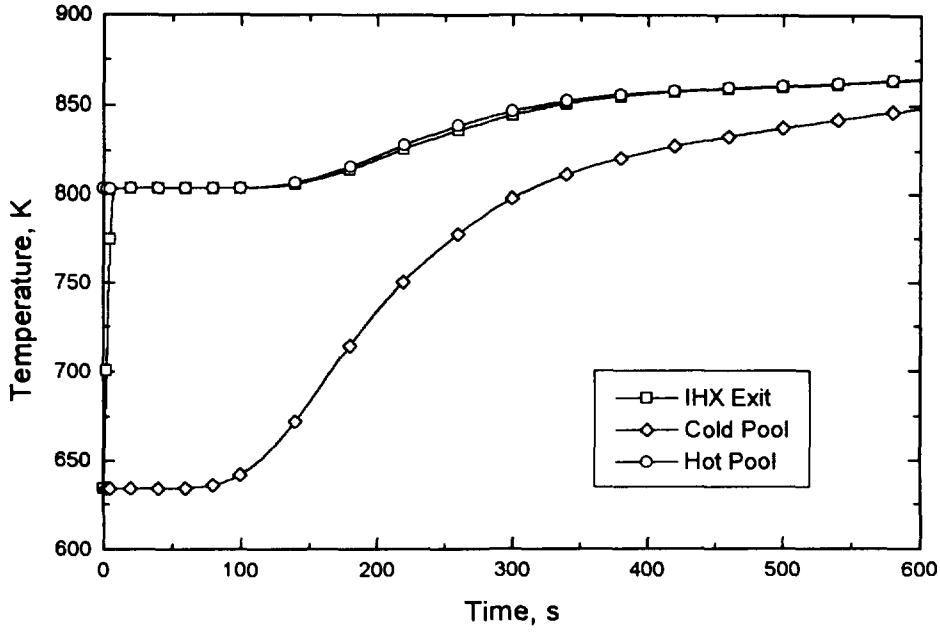

Fig. 4.8: Sodium temperatures

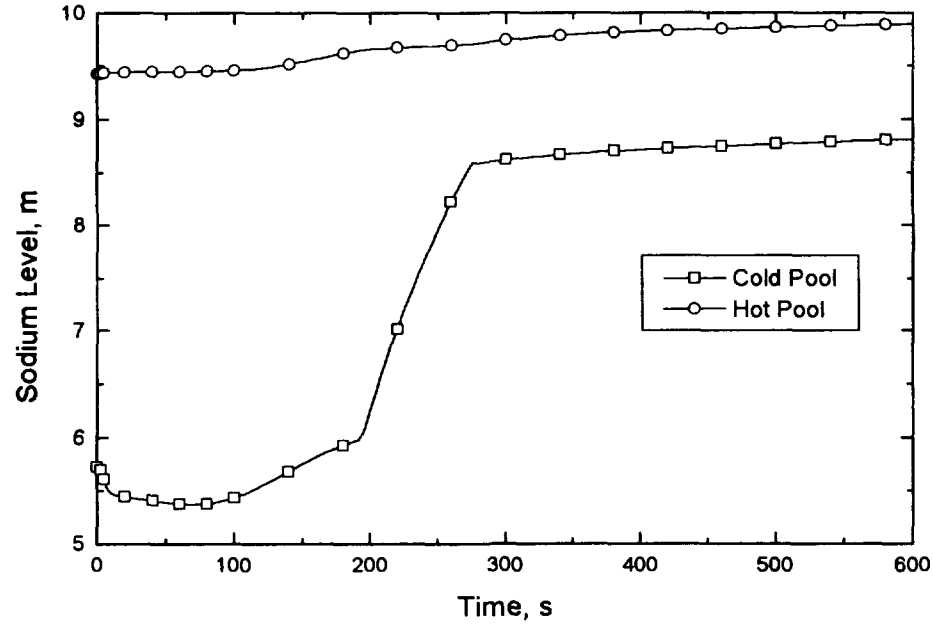

Fig. 4.9: Sodium levels

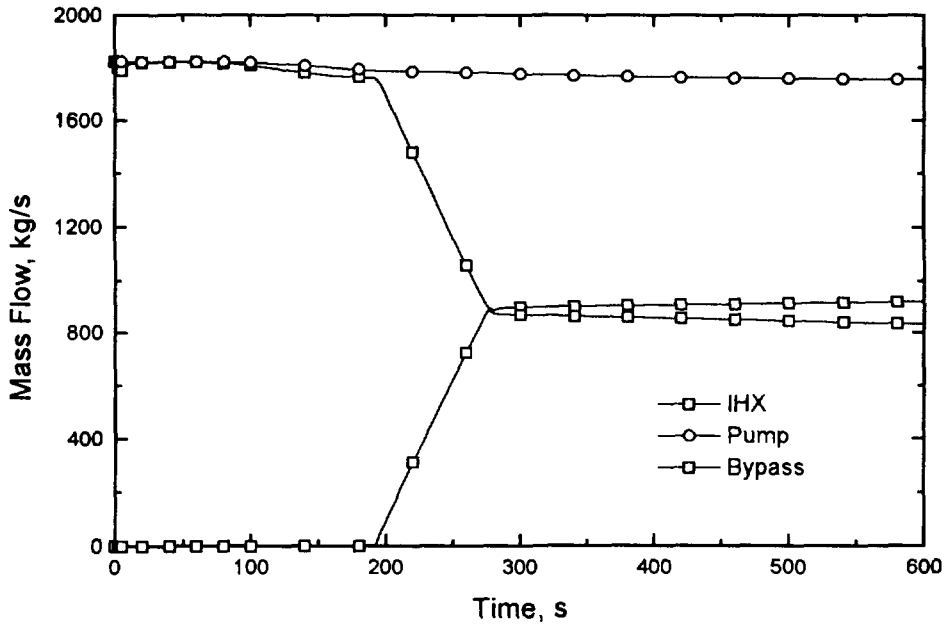

Fig. 4.10: Mass flow rates

4.2.3 Overflow/Break Simulation

The simulation has been performed to illustrate the simulation capability of SSC-K for the pipe break and the overflow transients during ULOHS accident. The pipes in the primary system exist only between pump discharge and core inlet plenum and are submerged in cold pool in pool-type LMRs. The value of the external pressure is much larger than that for loop-type design, which is generally equal to atmospheric pressure until the sodium in guard vessel covers the break location. This makes the pipe break in pool-type designs less sever relative to loop-type designs.

The transient was initiated by setting the heat transfer coefficient between primary and secondary systems to zero at 0 s and by assuming the pipe break in the pump discharge line at 10s. The primary pumps are assumed to operate normally, and the plant protection system is assumed not to scram the reactor. The height of the thermal barrier between hot and cold pools has been lowered same as the test run for overflow simulation.

Figure 4.11 shows the sodium temperatures at various locations. The trends are similar to ULOHS transient. The main difference is the increase rate of cold pool sodium temperature due to less core flow rate and larger cold pool sodium inventory. Figure 4.12 shows the sodium levels for hot and cold pools. As soon as pipe break occurs, the cold pool level starts to rise because break flow discharges to cold pool. At ~350 s, the hot pool sodium is flooded into cold pool and the cold pool sodium level rises more rapidly. As shown in Fig. 4.13, the pump discharge flow increases due to smaller pressure loss when pipe break occurs. The discharge flow from break reaches to some values and starts to decrease because of the increase of cold pool sodium level. As overflow starts to occur, the IHX flow rate decreases the same amounts of overflow rate.

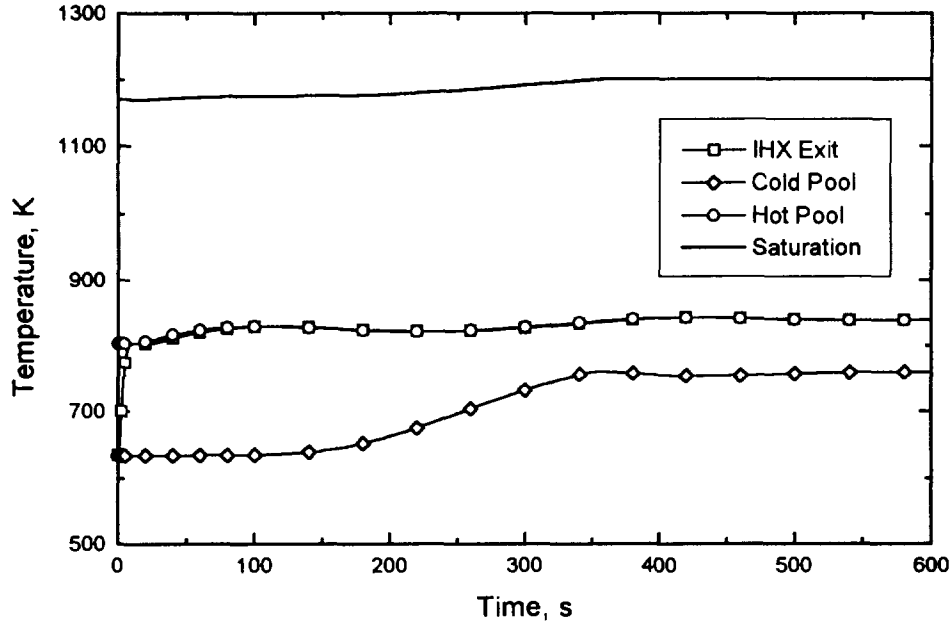

Fig. 4.11: Sodium temperatures

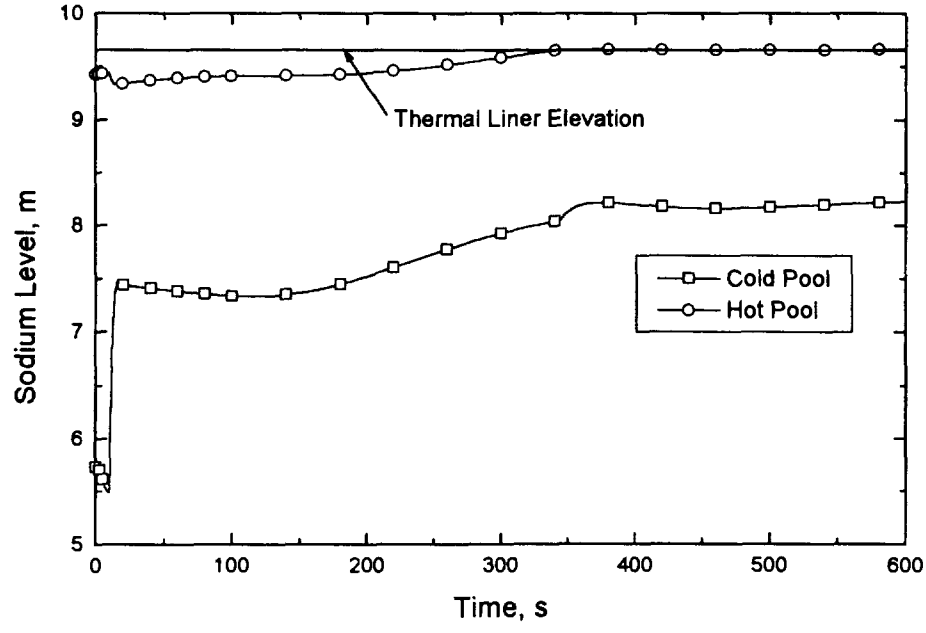

Fig. 4.12: Sodium levels

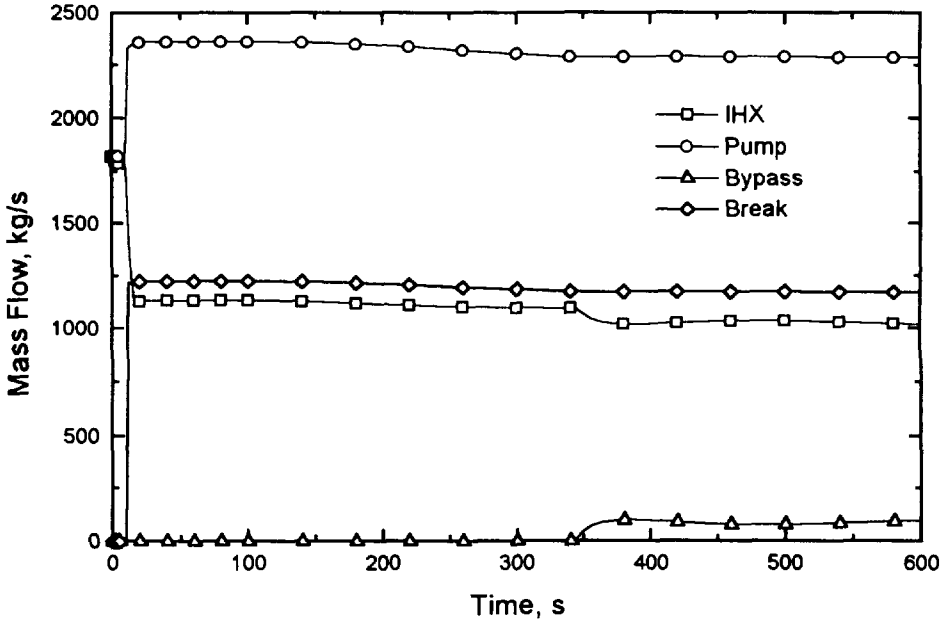

Fig. 4.13: Mass flow rates

5. Conclusions and Future Work

The best-estimate system code SSC-K for analyzing an variety of off-normal or accidents in a pool type design LMR has been developed on the basis of SSC-L developed at BNL to analyze loop-type LMR transients.

Because of inherent difference between the pool and loop design, the major modifications of SSC-L has been made for the safety analysis of KALIMER. The cold pool model has been developed by including mass and energy conservation equations for the cold pool region, which does not not exist in a loop-type LMR. In a pool-type LMR, the liquid in the hot pool can be flooded into cold pool and it forms the natural circulation flow path during the loss of heat sink transients. The momentum path has been added to calculate the flooding rate and mass and energy equations for hot and cold pools modified to account the mass and energy changes due to overflow. Since the pipes in the primary system exist only between pump discharge and core inlet plenum and are submerged in cold pool, a pipe rupture accident becomes less severe due to a constant back pressure exerted against the coolant flow from break. The break model has been modified to account the differnce of a pool-type LMR with a loop-type reactor. The steady state routine for initialization of plant initial condition has been modified to calculate the initial state of cold pool, i.e., sodium level, temperature, and mass.

Test runs have been performed for the qualitative verification of the developed models. However, the further validation of SSC-K is required to be used for the safety analysis of a real plant.

References

1. G. J. Van Tuyle, G. C. Slovik, R. J. Kennett, B. C. Chan and A. L. Aronson, "Analysis of Unscrammed Events Postulated for the PRISM Design," Nuclear Technology, 91, 165 (1990).
2. U. S. Nuclear Regulatory Commission, "Preapplication Safety Evaluation Report for the Power Reactor Innovative Small Module (PRISM) Liquid-Metal Reactor," NUREG-1368, (1994)

3. General Electric, PRSIM Preliminary Safety Information Document(PSID), (1986).

4. C. K. Park, et. al. "KALIMER Design Concept", *KAERI/TR-888/97.*

5. J. G. Guppy, et al., "Super System Code – An Advanced Thermohydraulic Simulation Code for Transients in LMFBRs," NUREG/CR-3169, BNL, (1983).

Appendix A. Input Changes

A.1 File VESSEL

RECORD 1

L6RTYP	Reactor type 1: Pool-type LMR
N6CHAN	Number of channels being simulated
N5RTYP	Number of rod types
N5ASEC(L)	Number of axial slices of each rod type (L=1, N5RTYP)
N5NFR(K)	Number of radial fuel nodes of each channel (K=1, N6CHAN)

RECORD 27

Z6REF	Reference elevation of reactor vessel [m]
Z6INOZ	Elevation of vessel inlet nozzle above Z6REF [m]
Z6BCOR	Elevation of bottom of core above Z6REF [m]
Z6TCOR	Elevation of top of core above Z6REF [m]
Z6UPLN	Elevation of initial upper plenum sodium level above Z6REF [m]
Z6ONOZ	Elevation of vessel outlet nozzle above Z6REF [m]
Z6UPTL	Elevation of top of thermal liner above Z6REF [m]
Z6VSTP	Elevation of top of vessel above Z6REF [m]

A.2 File NALOOP

RECORD 112

Z1HEDR	Rated head of primary pump [m]
U1OMGR	Rated speed of primary pump [RPM]
Q1FLOR	Rated volumetric flow rate of primary pump [m^3/s]
T1ORKR	Rated torque of primary pump [N-m]
Z1RTOT	Height of primary pump tank if L6RTYP ≠ 1 [m] Height of cold pool region from pump inlet to top of reactor vessel if L6RTYP = 1
A1RES	Cross-sectional area of primary pump tank [m^2]

Dummy value if L6RTYP = 1

Q1PYTQ Pump torque under pony motor operation [N-m]

V6BPMP Cold pool volume below pump inlet if L6RTYP = 1 [m^3]

Dummy value if L6RTYP ≠ 1

Z6IHXP Height from pump inlet to IHX exit if L6RTYP = 1 [m]

Dummy value if L6RTYP ≠ 1

A6IHXP Cross sectional area of cold pool region between pump inlet and IHX exit if L6RTYP =1 [m^2]

Dummy value if L6RTYP ≠ 1

A6OVRF Cross sectional area of cold pool region above IHX exit if L6RTYP =1 [m^2]

Dummy value if L6RTYP ≠ 1

RECORD 11YY : YY stands for pipe number of primary loop, YY = 0, N1PIPE

F1LOSS Loss coefficient for YY-th pipe in primary loop

X1PIPE Length of YY-th pipe in primary loop [m]

Y1PIPE Inner diameter of YY-th pipe in primary loop [m]

Note: For IHX, enter primary side hydraulic diameter.

Y1THIK Thickness of YY-th pipe wall in primary loop [m]

Note: This value is ignored for IHX primary pipe.

R1SIN(I) Angle of primary flow at each node in YY-th pipe of loop [deg], (I = 1, N1NODE(N1PIPE(YY)))

RECORD 8004 :

S8MANP(J) Time at which pumps are to be tripped manually [S] (J=1,(4*N1LOOP+1))

S8MANX(I) Time at which IHX are to be tripped manually [S] (J=1,N1LOOP)

Note: Parameters are assigned on a subsystem/component basis. That is, data assignments are made for the pump in primary loop 1, the pump in primary loop 2 (if needed), and so on, up to the pump in primary loop "N1LOOP". The data for all "N1LOOP" primary loop pumps is followed by corresponding series for the secondary loop(s) and each of two dummy steam generator pumps. Data for the last pump is assigned to the turbine. Pump trips for the steam generator and

turbine must be set through record 3401.

Note: Length of each node is calculated by X1PIPE/(N1NODE-1) instead of X1PIPE/N1NODE.

One half nodes of both ends of each pipe holds in common with adjacent pipe. Table below shows as an example by applying with sample input data.

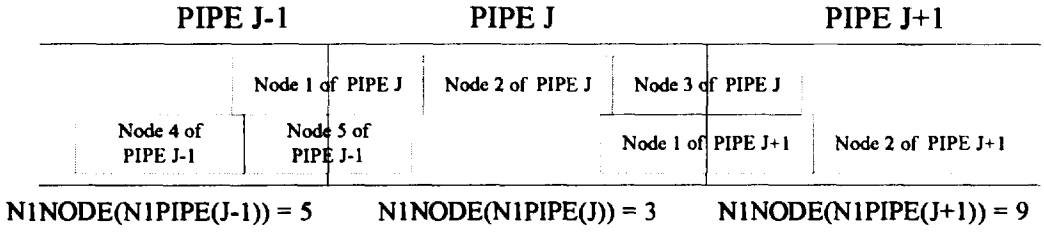

Fig. A.1: Pipes

- Sample Input

```
1101D 0.0, 0.6858, 1.13, 0.02, 0.0, 0.0/
1102D 0.0, 5.8674, 8.068E-3, 0.0, -90.0, 14R/
1103D 0.0, 1.397, 0.6572, 0.0190, -90.0, 5R/
1104D 0.0, 4.9276, 8.1175, 0.025, -90.0, 10R/
1105D 0.2, 5.4864, 0.94266, 0.051, -45.0, 4R, 0.0, 7R, 45.0, 4R/
1106D 0.0, 4.9276, 1.9283, 0.051, 90.0, 10R/
1107D 0.13, 4.963995, 0.58, 0.051, 90.0, 10R/
1108D 0.90, 10.8196, 0.8621, 0.051, 0.0, -90.0, 10R/
```

Table A.1: Elevation of Each Pipe Exit for the Primary Loop

PIPE No.	X1PIPE	N1NODE	DX	Height (Δ Z)	Elevation, m
Z6ONOZ : Elevation of vessel outlet nozzle					12.6644
1	0.6858	2	0.6858	0.0	12.6644
2	5.8674	14	0.451338	13*DX*SIN(R1SIN)=-5.8674	6.797

3	1.397	5	0.34925	4*DX*SIN(R1SIN)=- 1.397	5.4
4	4.9276	10	0.547511	9*DX*SIN(R1SIN)=-4.9276	0.4724
5	5.4864	15	0.391886	DX*SIN(R1SIN)=-0.277105	0.195295
6	4.9276	10	0.547511	9*DX*SIN(R1SIN)=4.9276	5.122895
7	4.963995	10	0.551555	9*DX*SIN(R1SIN)=4.963995	10.08689
8	10.8196	11	1.08196	9*DX*SIN(R1SIN)=-9.73764	0.34925
Z6INOZ : Elevation of vessel inlet pipe					0.34925

Appendix B. Code Modification List

Table B-1: Code modification List

Subroutine Name	Changes
CRDR9R	Inconsistent subroutine arguments: GENRD
DCODNC	Inconsistent data type with subroutine argument. • IVLU been set to real(8) from integer
END1T	Inlet/Outlet enthalpy of pipe segment in cold pool has been changed
EQIV1T	No pump surge tank option • head due to liquid level to zero • matrix element for head due to liquid level to zero • pump speed change rate to zero • liquid level change rate to zero Bypass flow calculation has been corrected Integrated values related to pool model has been changed
EQIV2T	No pump surge tank option • head due to liquid level to zero • matrix element for head due to liquid level to zero • pump speed change rate to zero • liquid level change rate to zero
ERRMSG	2nd argument of EXIT9U to 8 characters
FLOW1T	No pump surge tank option has been added
FLOW2T	No pump surge tank option has been added
GENRD	Inconsistent data type with subroutine argument. • IVLU been set to real(8) from integer
GVSL1T	External pressure for break flow calculation
HEAD1T	Discontinuity in pump head homologous curve removed
HYDR1S	Pressure drop calculations corrected
IHX1T	LOHS actuation at specified time by user
INIT1T	Initialization for no pump surge tank case • pump inlet pres. to vessel outlet pres. • head due to liquid level to zero Initialization for cold pool variables • Cold pool sodium mass • Pump inlet pressure Cover gas volume calculation

	Cold pool enthalpy calculation
INIT2T	Initialization for no pump surge tank case • Pump inlet pres. to preceeding pipe outlet pres. • Head due to liquid level to zero
INTG1T	Inconsistent data type with subroutine argument. • IVLU been set to real(8) from integer
ISETHM	Character variables can not be set to real variables directly. • Character variables are set to real variables using write statement.
LOOP1T	Cold pool enthalpy calculation
NSKIP	Inconsistent data type with subroutine argument. • IVLU been set to real(8) from integer.
PBAL9S	ERR9U arguments been changed • sequence of arguments has been changed
PIPE1S	Enthalpy and pressure drop calculation routine for cold pool added
PIPW1T	Pressure drop calculation routine for cold pool added
PRUP6T	Calculation for IHX inlet pressure been corrected
PUMP1S	Discontinuity of head homologous curve been corrected
PUMP1T	Discontinuity of head homologous curve been corrected EMP coastdown at specified time No enthalpy rise across EMP assumed
READ1R	GENRD arguments been changed : 19 places • 4th arg.: integer(id2) to real(d2)
READ7R	GENRD arguments been changed : 43 places • 4th arg.: integer(id2) to real(d2)
READ8R	GENRD arguments been changed : 1 place • 4th arg.: integer(id2) to real(d2) GENRD arguments been changed : 1 place • 3rd arg.: real(dum) to integer(idum) • 5th arg.: real(dum) to first real array element[a(1)] • 6th arg.: real(dum) to first int array element[ia(1)]
READ9R	int. array for data containment[ia(1)] been included GENRD arguments been changed : 7 places • 4th arg.: integer(id2) to real(d2)
READ9T	equivalence statement (A(1),IA(1)) been removed GENRD arguments been changed : 1 place • 3rd arg.: real(dum) to integer(idum) • 5th arg.: real(dum) to first real array element[a(1)] • 6th arg.: real(dum) to first int array element[ia(1)] GENRD arguments been changed : 3 places • 4th arg.: integer(id2) to real(d2) error message for excess of max. table length been removed
READHM	Character variables can not be set to real variables directly. • Character variables are set to real variables using write statement.
REPEAT	Inconsistent data type with subroutine argument. • IVLU been set to real(8) from integer.
RES1S	Steady state calculation for cold pool

RES1T	No pump surge tank option has been added • liquid level in pump tank to zero • pump inlet presssure to vessel outlet pres. • liquid level change rate to zero Cold pool option added • Time derivative of cold pool sodium mass • Cold pool level calculation • Pump inlet pressure
RES2S	No pump surge tank option • gas mass in surge tank to zero • liquid level in surge tank to zero
RES2T	No pump surge tank option • liquid level in pump tank to zero • pump inlet pres. to vessel outlet pres. • liquid level change rate to zero
RITE6U	int. variables HY, HI been defined definition for character STRING1 been changed
UPLS6T	• Overflow model added • Mass, energy equations changed to include overflow effect • Time derivative of enthalpy difference due to overflow modified
VERR9T	Dimension for character NAME been changed to character*6
VESL1T	Overflow rate calculation Cover gas volume
VRFY9T	character NC been defined VERR9T arguments been changed : 11 places • 4th arg.: integer(+0) to character(NC) VERR9T arguments been changed : 1 place • 4th arg.: null character to character(NC)
WIMPLT	Cover gas volume calculation

서 지 정 보 양 식

수행기관보고서번호	위탁기관보고서번호	표준보고서번호	INIS 주제코드
KAERI/TR-1266/99			

제 목 / 부 제
Pool 형 액체금속로용 열수력코드 SSC-K 개발
주 저 자 : 김 경 두 (칼리머 설계기술개발팀)
연구자 및 부서명
권영민, 석수동, 장원표, 한도회 (칼리머 설계기술개발팀)

출 판 지	대전	발행기관	한국원자력연구소	발행년	1999. 3.
페 이 지	p. 69	도 표	있음(○), 없음( )	크 기	29.7 cm
참고사항					
비밀여부	공개(○), 대외비( ), ___ 급 비밀		보고서종류	기술보고서	
위탁연구기관			계약 번호		

초록(15-20 줄내외)

SSC-K (Supper System Code of KAERI)는 Pool 형 액체금속로의 다양한 정상/비정상 조건 및 사고를 분석하기 위한 최적열수력코드이다. SSC-K 는 미국 BNL 에서 Loop 형 액체금속로의 안전해석을 위해 개발된 SSC-L 을 기반으로 개발되었다.

KALIMER 와 같은 Pool 형 원자로는 Loop 형 원자로와 근본적으로 설계개념이 상이하여 KALIMER 안전해석을 위해서는 Loop 형 액체금속로 안전해석을 위해 개발된 SSC-L 의 전반적인 코드 수정이 필요하다. KALIMER 와 일반적인 Loop 형 원자로의 주요 차이는 일차 열전달계통에서 나타난다. KALIMER 에서는 일차 열전달계통을 구성하는 모든 주요 기기가 원자로 용기내에 위치하나, Loop 형 원자로에서는 모든 주요기기가 원자로용기 외부에 위치하며 파이프를 통하여 연결되어 있다. 또한 KALIMER 는 일차계통에 하나의 가스 영역이 존재하여 일반적으로 Loop 형 원자로와 같이 가스영역이 펌프탱크와 상부동공으로 분리되지 않는다. KALIMER 는 고온풀과 저온풀이 절연판으로 분리되어 있어 고온풀과 저온풀이 수위가 다르다. 이는 유로에서의 압력강하 및 펌프의 수두에 의해 발생한다. 열제거 기능이 저하되는 사고 발생시에는 고온풀의 수위가 절연판 상부보다 높아져 저온풀로 넘치게 된어 자연순환유로가 형성된다. 이는 피동잔열계통과 같이 열제거 상실사고시 주 열제거형태로 작용한다. KALIMER 는 Loop 형 원자로와 달리 관파단 사고의 발생은 펌프배출파이프에서만 가능하고, 이 파이프도 저온풀에 잠겨 있어 파단유량은 감소한다. 중간 열전달계통과 증기발생기계통은 Loop 형 원자로와 일반적으로 동일하다.
위에서 지적한 Pool 형 원자로의 차이를 반영하기 위해 SSC-L 코드를 전반적으로 수정하여 Pool 형 액체금속로 안전해석에 적합한 SSC-K 를 개발하였다. 개발된 모델은 시험계산을 통하여 정성적으로 타당한 예측능력이 있음을 확인하였으며, 향후 KALIMER 안전해석에 사용할 수 있을 것으로 사료되며, 이를 위해서는 개발된 모델에 대한 충분한 검증작업이 이루어져야 한다.

주제명키워드 (10 단어내외)

액체금속로, 칼리머, 안전해석, 풀형, 열수력모델

BIBLIOGRAPHIC INFORMATION SHEET

Performing Org. Report No.	Sponsoring Org. Report No.	Standard Report No.	INIS Subject Code
KAERI/TR-1266/99			

Title / Subtitle	Development of Thermal-Hydraulic System Analysis Code SSC-K for Pool-Type Liquid Metal Reactor
Main Author	Kyung-Doo, Kim (KALIMER Design Team)
Researcher and Department	Y.M. Kwon, S.D. Suk, W.P. Chang, D.H. Hahn (KALIMER Design Team)

Publication Place	Taejon	Publisher	KAERI	Publication Date	1999. 3.
Page	p. 69	Ill. & Tab.	Yes(o), No( )	Size	29.7 cm
Note					

Classified	Open(o), Restricted( ), ___ Class Document	Research Type	Technical Report
Sponsoring Org.		Contract No.	

Abstract (15-20 Lines)

The Supper System Code of KAERI (SSC-K) is a best-estimate system code for analyzing an variety of off-normal or accidents of a pool type design. It is developed at Korea Atomic Energy Research Inititution on the basis of SSC-L developed at BNL to analyze loop-type LMR transients.

Because of inherent difference between the pool and loop design, the major modefications of SSC-L is required for the safety analysis of KALIMER. The major difference between KALIMER and general loop type LMRs exists in the primary heat transport system. In KALIMER, all of the essential components consisted of the primary heat transport system are located within the reactor vessel. This is contrast to the loop type LMRs, in which all the primary components are connected via piping to form loops attached externally to the reactor vessel. KALIMER has only one cover gas space. This eliminates the need for separate cover gas systems over liquid level in pump tanks and upper plenum. Since the sodium in hot pool is separated from cold pool by insulated barrier in KALIMER, the liquid level in hot pool is different from that in the cold pool mainly due to hydraulic losses and pump suction heads occuring during flow through the circulation pathes. In some accident conditions the liquid in the hot pool is flooded into cold pool and forms the natural circulation flow path. During the loss of heat sink transients, this will provided as a major heat rejection mechanism with the passive decay heat removel system. Since the pipes in the primary system exist only between pump discharge and core inlet plenum and are submerged in cold pool, a pipe rupture accident becomes less severe due to a constant back pressure exerted against the coolant flow from break. The intermediate and steam generator systems of both designs are generally identical.

To adapt SSC-K to KALIMER design, the major modification of SSC-L has been made for the safety analysis of KALIMER. Test runs have been performed for the qualitative verification of the developed models.

The present work would make it possible to use SSC-K for the priliminary safety analysis of KALIMER. However, the further validation of SSC-K is required to be used for real applications.

Subject Keywords (About 10 words)	LMR, KALIMER, Safety Analysis, Pool-Type, Thermal-Hydraulic Model